UCL Université catholique de Louvain

École polytechnique de Louvain (EPL)

Predictive Control of Grip Force and Learning of different Object Dynamics in Collision Task

Dissertation presented by

Laurane GUIOT

for obtaining the Master's degree in

Biomedical Engineering

Option(s): Biomedical data analysis and Biomechanics and medical robotics

Supervisor(s)

Philippe LEFÈVRE , Jean-Louis THONNARD, Florian SALMEN

Reader(s)

Michel VERLEYSEN, Frédéric CREVECOEUR

Academic year 2015-2016

Remerciements

La réalisation de ce mémoire n'aurait pas été possible sans l'intervention de plusieurs personnes à qui je voudrais témoigner toute ma reconnaissance.

Avant toute chose, je tiens à exprimer ma profonde gratitude et remerciements envers Messieurs Lefèvre et Thonnard qui m'ont donné la possibilité de terminer mes études par un travail riche et passionnant. J'aimerais également adresser mes sincères remerciements à Florian et David pour leur encadrement, leur aide et précieux conseils ainsi que leur disponibilié tout au long de l'année.

Je remercie également mes parents pour leur encouragements et leur support moral. Mes derniers remerciements iront pour toi, Thibaut, pour ton aide précieuse, ton soutien inconditionnel, ta patience ainsi que tes conseils avisés.

Contents

List of Figures

Chapter 1

Introduction

1.1 General introduction

Grasping movements are common tasks that we all used to practice. These tasks require precised and complex interactions with objects in our environment.

When objects are manipulated, the brain has to collect, analyze and stock a maximum data inputs concerning physical properties of the object as well as the environment within it interacts. Sensory information as tactile information and proprioception completed by visual feedback are crucial information for an efficient grasping. Tactile information can be obtained thanks to different mechanoreceptors spread all over the skin [1]. Indeed, one has to be able to provide an adequate force to grasp an object without dropping it and without damage it by overtightening. In addition, proprioception helps the grasping in an other way. It helps to be conscious of the position and movements of each body segment (position of a finger relative to the other, for example) and to unconsciously give to the nervous system the necessary information for the adjustment of contractions for muscle movement and maintaining posture and balance.

Some movements as holding a needle to take blood out or simply write with a pen force us to held objects with the precision grip. Precision grip is the way of grasping an object with the thumb and the index finger only, both opposed as represented on figure 1.1(a). When an object is grasped with precision grip the grip force develops a normal force in response to a load force, in order to avoid slipping and the drop of the object. The normal force applied by the subject on the grasped surface is called as grip force (GF). The resultant of tangential forces, including gravitational inertial forces at the interface digits/surface is called load force (LF). Moreover, the grip force is precisely controlled such that it is higher than the minimal grip force needed to avoid the object's slipping.

On figure 1.1(b), we can see that the grip force is synchronized with load force variations when an object is held. The grip force directly compensates the global load force, a combination

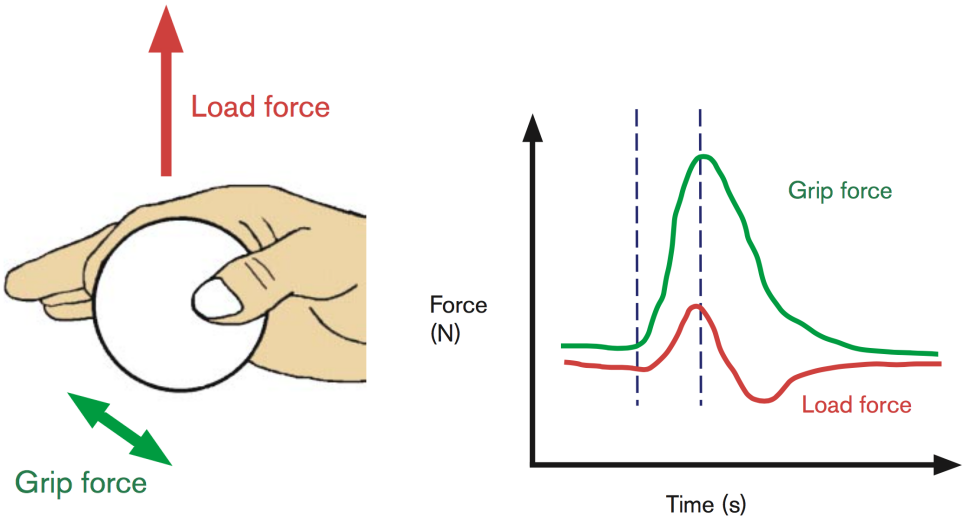

(a) Precision grip (b) GF and LF coupling

Figure 1.1: Grip and load force coordination [2]

of gravitational and inertial forces.

1.2 Internals models

In the particular field of objects manipulation, much data from different studies on coordination between reaching and grasping confirm the existence of an internal forward model [2]. Generally the models used to represent the neural process controlling the kinematics and the dynamics of the movement are called internal models. Such a system is termed internal as it is internal to the central nervous system (CNS) [3]. These models are a way to represent neuronal processes used to compare motor commands and estimating their consequences.

The motor system is controlled by continuous interactions between the limbs and internal models. Nowadays, two types of internal models are listed ([2],[3],[4],[5]):

1. The internal forward model which can predict sensory consequences based on copies of outgoing motor commands, called efference copies.

2. The inverse model which can estimate motor commands based on desired trajectory information.

The synchronization between grip and load force represents a significant evidence for an internal model. This coupling is explained by a structure comprising both and internal forward model and an internal inverse model of the arm, as we can see on figure 1.2.

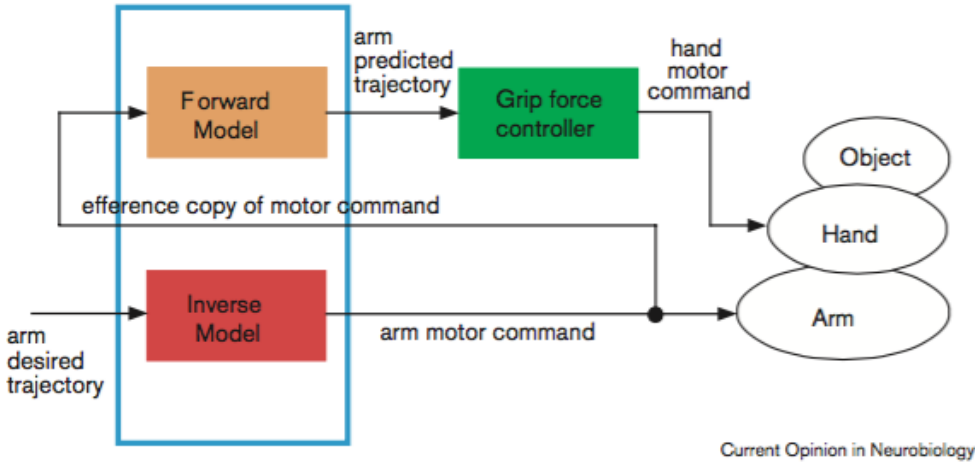

Figure 1.2: Computational model based on internal forward and inverse models [2].

One can see that motor commands sent to the muscles of the arms, hand and fingers in order to produce the desired movement are the output of the inverse model. Conversely, an efference copy of the motor command is sent to the forward model in order to predict the arm trajectory. This predictive trajectory is finally used by the grip force controller to produce the needed grip force to the object's manipulation. The grip force is thus predictively controlled thanks to a forward model.

The main advantage of feedforward control is the fact that it can anticipate the desired action without waiting for feedback control. Indeed, if the control of the grip force was only based on sensory feedback, the grip force would not be synchronized with the load force because of the sensorimotor delay, varying from 20 to 80ms, according to the speed of the sensory afference [2].

The anticipatory adjustment control of grip force with load force during object manipulation has been largely studied to provide evidence of forward models, as it has been explained above. Also, when a movement is self-produced, for example when the load at the fingertips periodically varies as according to this self-generated, the grip force decreases and increases in parallel with load force [6]. The sensory consequences can be accurately predicted, and this prediction can be used to attenuate the sensory effects on the movement [7]. Furthermore, evidence suggests that the cerebellum might be involved in generating the prediction of the sensory consequences of movement [7].

All this confirms the importance attached to the predictive system, allowing the grip force modulation with respect to predictable load force fluctuations. Three elements are retained to be significant to the grip and load force coupling on the computational model represented on figure 1.2:

- The inverse model (in red) in order to reach the target with arm,

- The internal forward model (in orange) to predict the arm trajectory,
- The grip force controller (in green) to control the grasping force

It is important to know that internal models are not fixed entities. The latter can be learned and updated through experiences. Therefore, predictions errors due to comparison of the predicted motor command and actual motor command can updated and improved an internal model [3].

1.3 Predictive and reactive grip force control

In everyday life, sudden load force changes when handling object happen frequently. For example, when handling as bag which suddenly falls down or simply when we get rushed when handling a glass filled with water. These sudden load changes can be predictive or not, depending if the perturbation may be anticipated or unexpected and depending on the capacity of the motor behavior to adapt itself by minimizing these perturbations. The ability of precision grip to adapt itself from this rapid load changes has been extensively investigated by different studies [8]. The precise coordination of thumb and index finger is provided by the movement prediction generating an adequate grip force in addition to the ability of updating this prediction via reactive mechanisms [9].

When the load change is predictive, the grip force increases in parallel with the load force. However, the grip force starts to slightly increase before the collision ([9],[10], [11], [12], [13]). Such an increase of grip force before the impact indicates an anticipation of load force changes. Indeed, this was taken as evidence of the existence of internal forward model of the arm and manipulated objects.

Parallel changes of grip and load force were also observed in point-to-point movements where load forces fluctuations came from inertial forces or others [14]. In that study, it also has been proved that grip force was modulated with load force variations. More interestingly, it has been shown that during horizontal movements, the pattern grip force/load force differs slightly, possibly due to load force variations.

When load changes suddenly, an increase of grip force has been observed just before the impact, which evidenced a predictive force control. When these changes become non predictive, that is to say reactive, studies have showed that grip force value largely overcame the load force value and that grip and load force profiles were decoupled ([11],[12],[14]). At the impact, the load force increases rapidly, whereas the peak of grip force occurs after the peak of load force [13], [12]. However, in a recent study [9] where participants were asked to keep an object in precision grip while an attached mass was dropped, authors found that subjects still reach a peak of grip force

after the expected impact in a blank trial (no collision and therefore no load force changes occur).

The question about the presence and nature of this delayed peak of grip force was asked in many studies. In some studies ([15], [9]) it has been concluded, thanks to blank trials experiments carried out in a virtual environment, that this peak was essentially preprogrammed and not reactive to the collision. One hypothesis would be that the central nervous system (CNS) optimizes the stability in objects manipulations by regulating mechanical parameters, included stiffness and damping through the grip force. Therefore, it would seem that the nature of this peak is essentially predictive [9].

1.4 Sensory information

Information provided by somatosensory system has its importance for grip force control. It is thanks to the tactile and visual feedback as well as proprioception information that an efficient grasp during dexterous manipulation is determined. Note that the sensory feedback is used to correct errors which are caused by an appropriate motor command. It evaluates the discrepancy between the actual and desired state. Not having a mechanical feedback would mean having a perfect internal model, which is impossible [16].

When we experience a first contact with a novel object, information about the nature and dynamics are given by the mechanoreceptors. There are four types of mechanoreceptors and they differ from their receptive fields and their nerve impulse speed. To summarize the tactile sensing, the object comes into contact with the skin and leads to a distortion of the skin inducing another distortion of the sensory receptors embedded in the skin. Following this, a neural signal is transmitted to the brain and decoded. This process provides a perception of tactile information [17].

During all that manipulations, it has been shown that the haptic sensation can improve the adaptation of grip force. Indeed, knowing the dynamic, surface properties and load of the object by its contact, helps to adapt our grip force prediction [1] [18]. In addition, visual feedback must also be taken in account in the prediction system. Some studies [19] wanted to evaluate the contribution of haptic feedback when learning to manipulate non-rigid objects. The second aim was to evaluate the way in which learning without haptic feedback affects the subsequent learning with haptic feedback and vice versa. Authors concluded that haptic feedback as well as prior experience with haptic feedback enhances the capacity of non-rigid objects control. A forward command is then based on internal model of object's properties (mass, friction, form,..). This is what we will call sensory memory. This memory allows the conservation of sensory impressions after manipulating object. The grip force adjustment to object's properties reflects the predictions based on the sensory memory of the previous manipulation [20].

1.5 Motor learning and adaptation

Learning involves changes in behavior due to interactions with the environment. It consists in a combination of motor and cognitive processes related to experience that lead to permanent changes in motor executions [16]. Motor control system must be able to maintain and update internals models. Its goal is to increases performances of movements, to make them more accurate and smoother which is necessary in everyday life. Motor learning can be viewed as the acquisition of forward and inverse internal models appropriate for different tasks and movements [21]. However, a difference must be made between learning control and adaptation control. Motor adaptations are represented by the temporary processes that affects the motor behavior during practice whereas motor learning refers to acquiring the ability to perform an action which can be considered as permanent [16]. This difference is important to understand for the results that will be presented and analyzed.

1.6 Aim of the work

This work will focus on the grip force adjustment during horizontal bimanual passive collisions. Recorded experimental data will allow us to analyze the predictive components of grasping in response to collisions. In other words, we want to know how timing and intensity of grip force adjusts predictively to novel object dynamics. The objective is also to observe an eventual learning of grip force through collisions. Moreover, thanks to this experimental model, it will be possible to analyze the effect of different intensities of impact as well as effects from previous trials on grip force adaptation.

The task will be executed on a new device composed of a manipulandum fixed at each handles situated at the end of a robotic arm. The experiment will contain several targets of different mass and stiffness that will be automatically launched towards one of the two hands of the subject. The subject will hold a manipulandum in each hand. Targets will carry out several collisions in a row, from one hand to the other before changing its mass and/or stiffness. In total, six collisions will be executed with the same target (three towards left hand and three towards right hand), and thus the same mass and stiffness before switching.

Chapter 2

Methods

2.1 Materials

A Kinarm robot shown on figure 2.1(a) is used to realize the experimental tasks. The end-point robot $Kinarm^{TM}$ is a robot composed of two mechanical arms with a vertical handle at the end of each arm. The robot is able to create complex virtual mechanical environments. It also includes of a virtual reality display whereby the user will execute the task. Moreover, a new function has been added to the handles. Two force sensors similar to a manipulandum will record the grip and load force of each hand (see figure 2.2(a)). These sensors will measure both the index and thumb grip force. The force sensors of the right and left handles have been correctly calibrated [22].

The subjects are sitting in front of the robot as shown in figure 2.1(a). They can control the two handles of the robot, one in each hand, in order to move the cursor on the horizontal mirror. After the calibration of the robot's arm position, the cursor is thus reflecting the hand position of the subject. In order to only have the position of the cursor on the horizontal mirror, a cover will be disposed behind the mirror. Subjects will thus have the cursor of the handles providing them visual feedback.

The robot controls the position and movements of the hands. A force sensor allows to measure the force exerted by the subject on the robot's handle. Forces and torques sensors of the Kinarm robot (see figure 2.1(b)) have six degrees of freedom. It is thus possible to know the magnitude of forces and torques in all directions.

The system is composed of an experimental control software and hardware called $Dexterit\text{-}E^{TM}$ and of a library created in the Simulink environment of Matlab as well as a Stateflow toolbox in order to code a task program [23]. Data acquisition is done at 1kHz and the robot is controlled by a real time computer executing precisely the program of the experimental protocol.

(a) End-point robot Kinarm

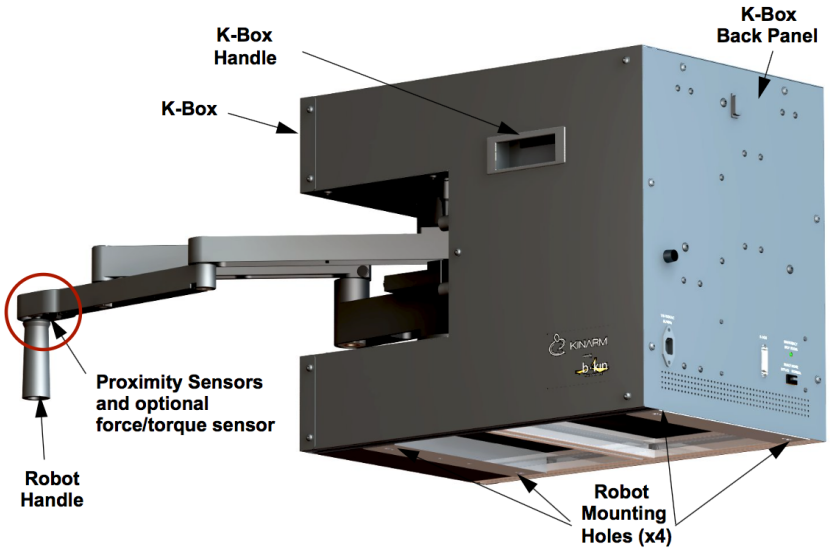

(b) Kinarm sensors (in red)

Figure 2.1: Representation of Kinarm End-point robot

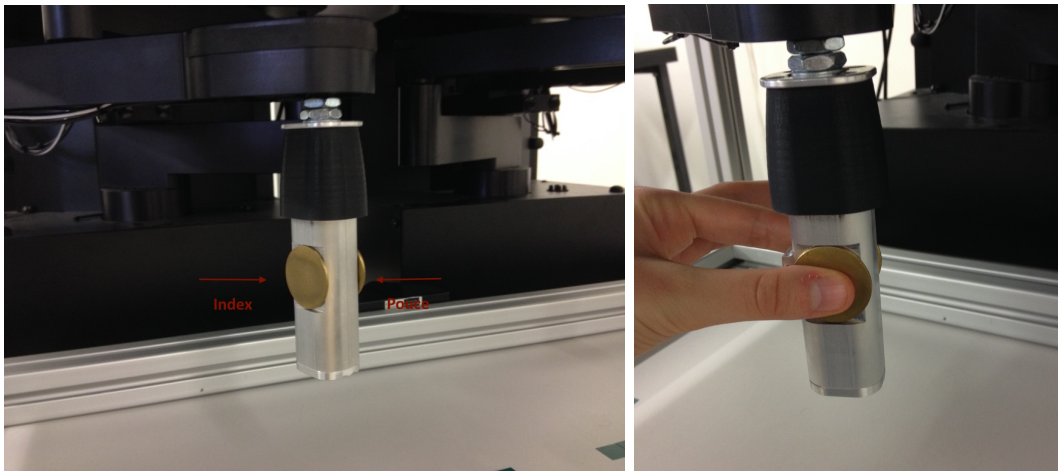

(a) Grip and load force sensor of the precision grip (b) Fingers position for the left handle

Figure 2.2: Representation of the new device installed on the robot handles. The handle represented is the left one.

2.2 Subjects

The 19 subjects who participated in the experiment were aged from 18 to 60 years. In total, there were 11 women and 8 men. These subjects were separated in two groups. One group began the experiment with the first collision on the left hand and the other one on the right hand. All participants did not report any motor disabilities and all of them gave their informed consent to participate in this experiment.

2.3 Experiment

2.3.1 Experimental set-up

We asked to the subjects to perform bimanual passive collisions with a automatically launched target towards the virtual representation of their hands. Subjects are given the instruction to hold their respective handle in their hands and to properly position their thumb and their index in face of their respective sensor (see image 2.2(b)). When the target will reach the hands of the subjects, they will pinch the handle in order to hold the handle as much as possible on the same position. Following this, the target will return in the opposite direction. Throughout the experiment, the position of two fingers on the sensors will be checked so as not to distort the test and thus to be able to acquire coherent data.

The experimental set-up is presented in figure 2.3. The global coordinates of the virtual representation, viewed by the subjects are defined with the x axis, positive to the right and the Y axis, positive towards the front. The origin (0,0) is defined at the center of the bottom of the screen perceived by the subject. The robot handles are represented by a green rectangle of

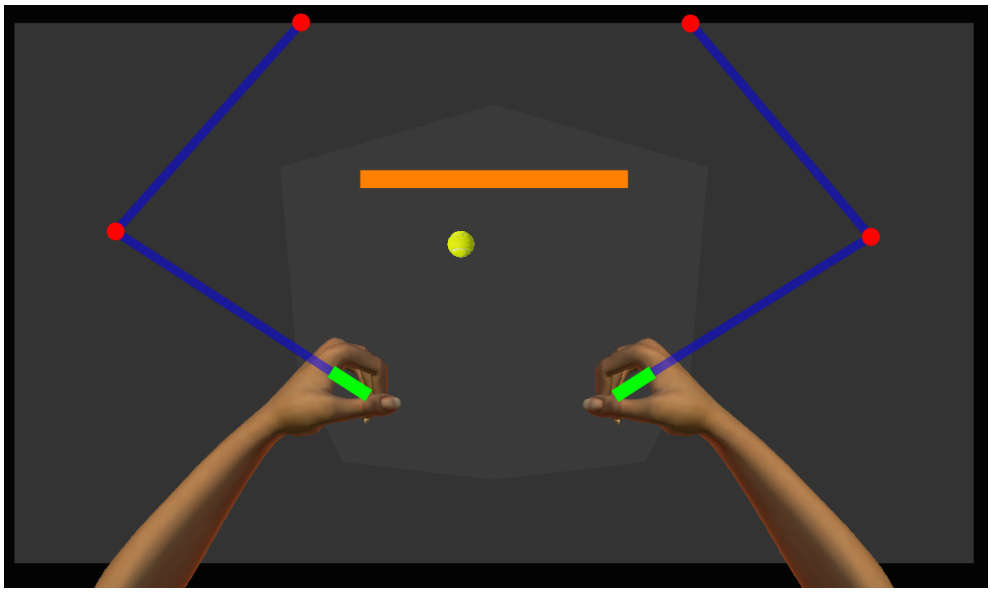

Figure 2.3: Experimental set-up

9 cm length and 1.5 cm width, inclined by 32.66 degrees each. These handles are separated by 30 cm. A horizontal wall is used for indicating the starting point of the target and is placed at 43 cm in y-direction. In this way, the target will have a diagonal direction. The target will be represented as a tennis ball of 3 cm diameter and launched with an initial velocity of 30 cm/s.

2.3.2 Experimental protocol

The experimental protocol takes place as follows: participants sit comfortably sit on a chair in front of the robot, looking at the mirror reflecting the virtual space with which they will interact. At the signal given by the experimenter, subjects should correctly grasp the manipulandum located on the handle of the robot with the thumb opposite to the index for each hand, both placed in the middle of the surface sensors. The fingers are aligned such that their axis is perpendicular to the representation of the handle, itself inclined at an angle of 32.66 degrees with the horizontal x-axis. The angle of 32 degrees was not chosen arbitrarily. A series of pre-test was experimented to find a comfortable enough angle to the subjects and leading to usable grip force traces.

For each trial, the instruction will be the same: after a defined time, the target will move either towards the left hand, or towards the right hand of the subject. Therefore, the task will to catch up passively and respond reactively as well as predictively to the collision of the target so that the handle moves as least as possible. The target will be repelled in the direction where it came from.

Three different masses targets were chosen as well as two different degrees of stiffness namely a spring constant k_1 representing a soft material and a spring constant k_2 representing a stiff

material. The values of k_1, k_2 are respectively set at 1000 N/m for the soft objects and 6000 N/m for the rigid ones. The three masses of the target m_1, m_2 and m_3 are set at 2kg, 4kg and 8 kg, respectively. The values are listed in the table 2.1. As for the angles, these values of mass and spring constant were selected after a series of pre-test, so as to obtain real and different collision dynamics from each other.

The target has a circular diameter of 3 cm and keeps the same shape throughout the experiment to eliminate any visual feedback with respect to the object properties. The only visual feedback of the participants is the visual feedback with respect to the direction and position of the target which allows the subject to anticipate the collision.
There are six different dynamics of collisions due to the masses and degree of stiffness. These experimental conditions are listed in table 2.2.

	k_1	k_2
m_1	2kg, 1000N/m	2kg, 6000N/m
m_2	4kg, 1000N/m	4kg, 6000N/m
m_3	8kg, 1000N/m	8kg, 6000N/m

Table 2.1: Experimental values

Experimental conditions			
Conditions	Pairs	Mass	Stiffness
1	m_1,k_1	light	soft
2	m_1,k_2	light	stiff
3	m_2,k_1	medium	soft
4	m_2,k_2	medium	stiff
5	m_3,k_1	heavy	soft
6	m_3,k_2	heavy	stiff

Table 2.2: Experimental conditions

Thirty series of six trials are performed within a condition (see figure 2.4). The repetition of trials allows 6 consecutive collisions namely three collisions with the left hand and three others with the right hand. For all subjects, the 6 conditions will be randomly distributed in order to have a non predictable first collision.

Between collisions in a same condition, the target will wait 50ms before being automatically launched towards hands. This time will increase to 1500ms between the different conditions. This will mark an indication for the subjects on changing physical object without knowing the

dynamic and physic of the next collision.

The experiment takes place in two blocks. The first block is composed of 15 series of 6 conditions (see table 2.2) with the first collision on the left hand. The second block is also composed of 15 series of the same 6 conditions but the first collision occurs on the right hand. According to the two groups of participants, one group will start with the first block followed by the second block and the other group will start with the second block followed by the first block.

Finally, 20% of "catch trials" were (pseudo)randomly added to the experiment in which the elastic force simulating the target collision was not applied [15]. We could therefore clearly measure the predictive grip force component. In others words, there would be one catch trials for 5 collisions.

The experiment lasts 40 minutes. Participants will have 3 breaks of 2 minutes to reduce fatigue effects.

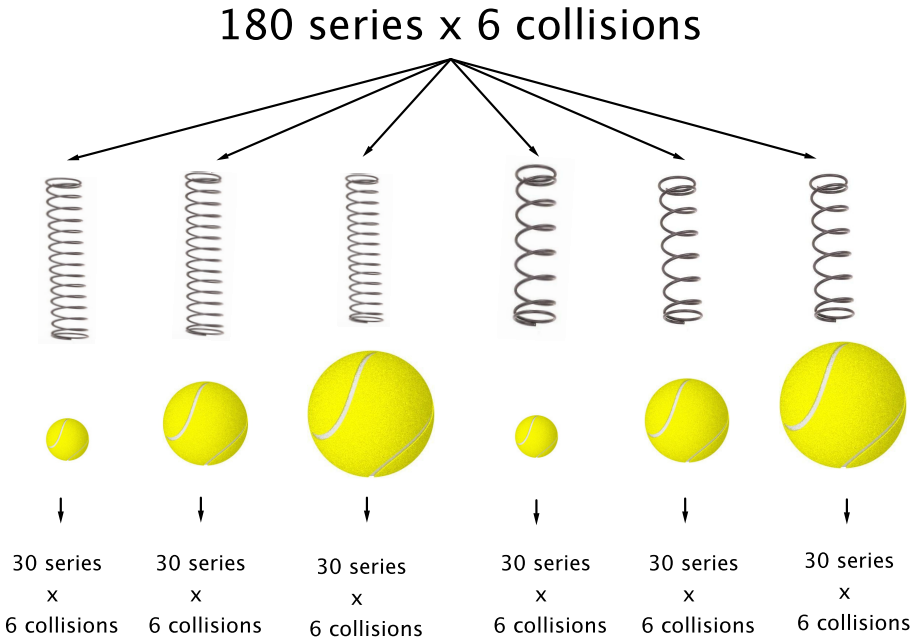

Figure 2.4: Experimental protocol composed of 30 series of 6 collisions for the six different conditions. This scheme represents the experimental protocol for each subject.

2.4 Data processing

Grip force and load force have been recorded with the KINGRIP Precision Grip Force at a sampling rate of 1 kHz. Let GF_{index} be the index grip force and GF_{thumb} the thumb grip force,

the total grip force has been computed as:

$$GF_{tot} = \frac{GF_{index} + GF_{thumb}}{2}$$

The total load force has been likewise computed :

$$LF_{tot} = \frac{LF_{index} + LF_{thumb}}{2}$$

In the experiment, all trials were aligned to the time of impact and the baseline of GF and LF was exerted from the data.

Integral of the load force is computed on an interval $[a, b]$. The limits a and b of the integral are respectively the value of point corresponding to 10% of the value of maximum peak load force and the value of point corresponding to 10% of the maximum load force peak after this peak. An example of these limits is shown on appendix figure A.1(a).

To compute the time when subjects start to grasp, two lines fitted on the curves of thumb and index grip force profile are used. The fit of the first line is based on the first values of the curves and the fit of the second line is fitted on the slope of the curve before impact. These two lines are represented on appendix on figure A.1(b). The time of the anticipation of grip force is taken at the intersection of these two lines. The value of grip force at the anticipation is thus the value of grip force at the anticipation time.

2.4.1 Linear regression

For the analysis of the results, we used a linear regression that predicts the predictive component of a grip force profile. What would be the grip force profile if it has been a catch trial? According to a study [15], the grip force maximum (GF_m) could be predicted with a multiple regression based on the grip force before contact (GF_c) and its derivative (dGF_c/dt). The same principle can be used to predict the moment when the peak of grip force (T_{GF}) will occur:

$$GF_{max} = \alpha_m GF_c + \beta_m \frac{dGF_c}{dt} + \gamma_m, \tag{2.1}$$

$$T_{GF_{max}} = \alpha_t GF_c \ + \beta_t \frac{dGF_c}{dt} \ + \gamma_t \tag{2.2}$$

To build this linear regression, the mean of all catch trials of one subject for each condition was computed. One example of the average catch profile of the heavy/stiff condition is shown on figure 2.5(a), in dark blue. With this average catch profile, two pairs of three coefficients α,β and γ per subject and per condition can be computed thanks to the following equations:

$$\underbrace{\begin{bmatrix} GF_{c_1} & \frac{dGF_{c_1}}{dt} & 1 \\ GF_{c_2} & \frac{dGF_{c_2}}{dt} & 1 \\ \vdots & \vdots & \vdots \\ GF_{c_n} & \frac{dGF_{c_n}}{dt} & 1 \end{bmatrix}}_{\mathbf{A_{max}}} \underbrace{\begin{bmatrix} \alpha_m \\ \beta_m \\ \gamma_m \end{bmatrix}}_{\mathbf{x_{max}}} = \underbrace{\begin{bmatrix} GF_{m_1} \\ GF_{m_2} \\ \vdots \\ GF_{m_n} \end{bmatrix}}_{\mathbf{b_{max}}}$$

$$\underbrace{\begin{bmatrix} GF_{c_1} & \frac{dGF_{c_1}}{dt} & 1 \\ GF_{c_2} & \frac{dGF_{c_2}}{dt} & 1 \\ \vdots & \vdots & \vdots \\ GF_{c_n} & \frac{dGF_{c_n}}{dt} & 1 \end{bmatrix}}_{\mathbf{A_t}} \underbrace{\begin{bmatrix} \alpha_t \\ \beta_t \\ \gamma_t \end{bmatrix}}_{\mathbf{x_t}} = \underbrace{\begin{bmatrix} T_{GF_{max_1}} \\ T_{GF_{max_2}} \\ \vdots \\ T_{GF_{max_n}} \end{bmatrix}}_{\mathbf{b_t}}$$

Then the two systems were solved by $x = A \setminus b$, and the three coefficients for each system were found to predict the maximum of grip force and its time after the collision. To obtain the predicted profile of grip force, we individually scale the x-axis of the mean catch with the predicted time and scale the y-axis with the predicted maximum grip force (see equation 2.1 and 2.2). One example is provided on figure 2.5(b).

To assess the accuracy of the predicted values, the mean of these values and the mean of the catch trials profiles were calculated. The two traces are very similar which indicates a good prediction of the values.

2.4.2 Statistical analysis

In the experiment, paired t-tests were used to investigate differences between results. For the learning part, we perform a multiple comparison test. A multiple comparison test enables to determine which pairs of group means are significantly different. The value R reported in the text is the correlation coefficient of two random variables which is a measure of linear dependence between two variables.
Values reported in the text are mean± standard deviation or standard error of the mean according to the results. The statistical analysis was done with Matlab.

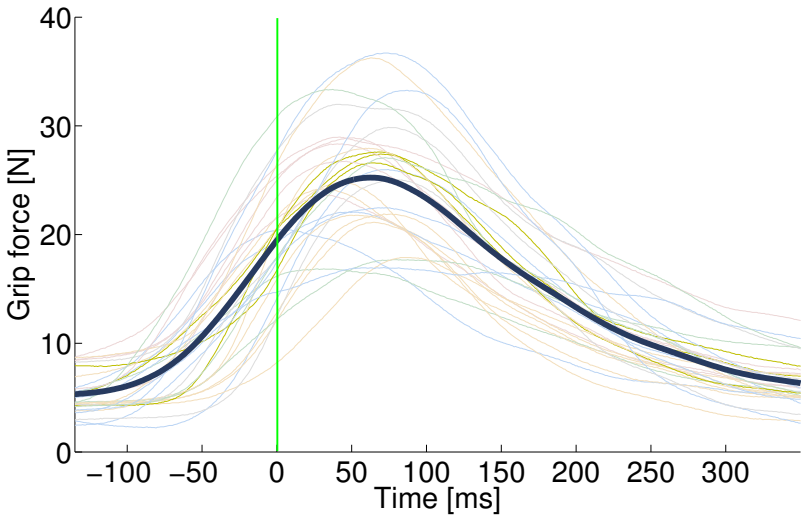

(a) Profil of the mean of all catch trial for one subjects in the heavy/stiff condition

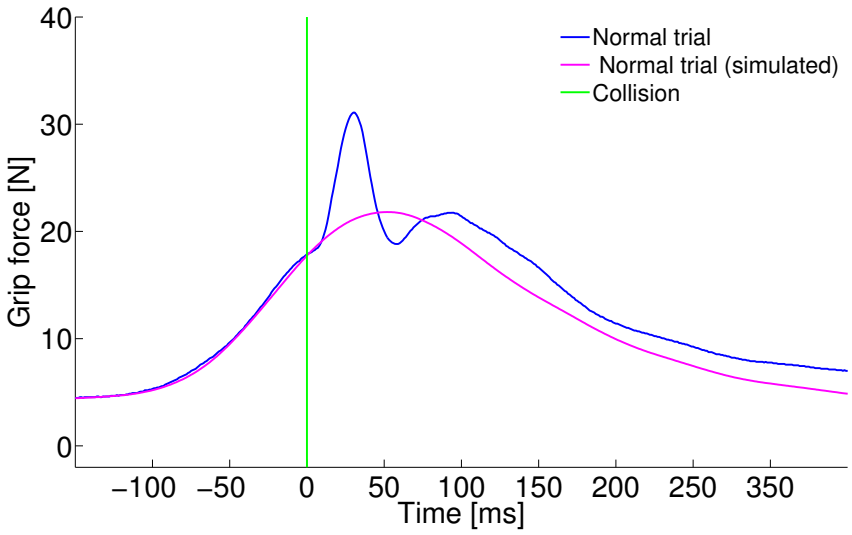

(b) Single collision for the heavy/stiff condition

Figure 2.5: a) Example of the mean (black curve) of all catch trials for one subject. b) Example of one trial. Blue curve is the thumb grip force. Pink curve is the allure that normal trial would have if it has been a catch trial. For the two figures, green line represent the moment at the impact (0 ms).

Chapter 3

The Programming Environment

3.1 Task program

Dexterit-E is a behavioral control and data acquisition software that operates KINARM Labs. This software is used to create small programs that define and control the system behavior that can occur during a single trial of a task, called Task program.

Mathworks' Simulink and Stateflow toolboxes are involved in the task program programmation. Simulink is a block diagram environment for multidomain simulation and a graphical programming environment in which Task Programs are developed. It is a graphical representation of data flow in the task [24], [25].
Stateflow is a modeling environment and logic simulation of combinational and sequential decision from state machines and flow charts [26]. Indeed, event-driven state machines called Stateflow Charts are developed by this graphical design tool.
A Stateflow Chart is a form of flowchart in which independent system states are created and Stateflow events are defined to allow transitions between those system states[24]. There are many of pre-made functions and blocks in Simulink. The own library of Simulink of BKIN Technologies is provided its own library of Simulink blocks. This library is specific to Dexterit-E's Task Programs. The main reason to use Simulink and Stateflow is to provide a stable programming environment with as much flexibility for the end-user as possible[24].

3.2 Stateflow chart

The figure below shows a flow chart version of what will happen during a single trial of the task. The Stateflow chart named `Trial_control` described above is included in a Simulink environment as shown in **figure** 3.2. Following the diagrammatic conventions of Stateflow, states are represented by ovals, transitions between states are represented by arrows, and small circles known as 'connective junctions' provide a way to connect multiple transitions together between states [24].

The task description is quite simple: For the first group of subjects beginning with the first left collision, the target has to move first toward subject's left hand. Inversely,for the second group, the target has to move first toward the right hand of the subjects. The task can be summarize in the steps shown on figure 3.1 :

1. The first step is the initialization step. When the Task Program is loaded, it needs to enter a default state. This step takes place to ensure that the target is initially off.

2. The second step consists of choosing the right and left target following the number of the active trial. If the latter is odd, target 1 is chosen, if it is even, target 2 is chosen. The difference between these two targets differs only in x position. One is positioned on the left side of the virtual representation, the other is placed on the right side.

3. After choosing the correct target the start target turns on which are the targets wherein subjects must position his hand before the beginning of the trial. Thanks to this, all subjects will place their hands in the same place throughout the experiment.

4. After the third step is completed, the main target will wait 1500 ms before moving. Note that, for the first collision the target wait 1500ms to mark a transition between series of different condition (heavy/stiff, light/soft,..). The target will just wait 50ms between collisions inside a same condition.

5. The target can start to move towards the correct hand and wait for collision.

6. The following step is to activate collision loads. It the target moves toward the left hand, the collision load force of the left hand will be activated at the contact between the left hand and the target and inversely. In addition, if the trial is a catch trial, the load force at the two hands will be deactivated.
   Moreover, the number of right and left collision is counted.

7. This leads us to the final step which is the loop towards the first step. The operation will carry out and also start again at the first step. If the number of collisions turns to 6, the program will notify us that will be the end of a series of the six collisions.

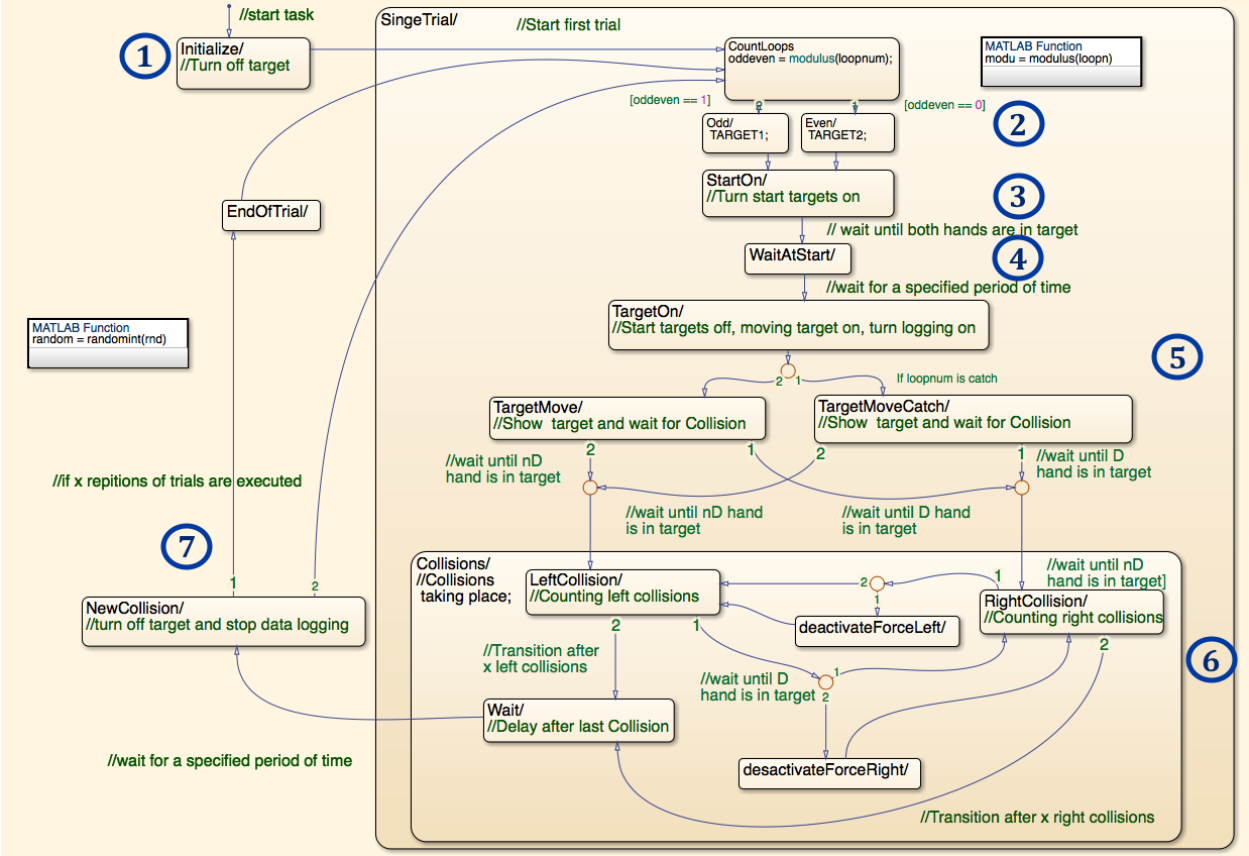

Figure 3.1: Stateflow flowchart during a single trial of the task

3.3 Simulink

The mains blocks of Simulink required by Dexterit-E must be added in the Simulink model. Among these bloks, the **GUI Control** block which takes care the communication between the Task Program (which runs on a real-time computer) and the Dexterit-E GUI (which runs on a separate, Windows-based computer) [24]. Its main function is to control the timing and sequence of trials and to output the appropriate Trial Protocol for each trial. It receives feedback from the Stateflow chart. As explained above,the Stateflow chart controls the behavior of the system during a single trial.

The various inputs use for the Stateflow charts provide data which can be used to drive the Stateflow chart [24]. In our case, the inputs are :

- The right and the left force of the arms
- The `KINARM_HandInTargetblock` provides feedback about which targets the hand is in. The indication if the hands are in the target `HandInTarget`.
- The parameters as time occlusion, waiting time,..
- The `Trial_protocol`

Stateflow chart also provides outputs that can be used to drive external Stateflow. These outputs will be used by the computer to run on real time the experimental task on the Kinarm robot. The main outputs used by the different blocks in Simulink are the following

- `Logging_enable` which is connected to the data logging block. The block logs all data to be saved by the Task Program, including KINARM-related data (i.e. position, velocity, etc.) as well as Task events. Data logging only occurs when the `logging_enable` input is set equal to 1 and the trial is running[24]

- `Events_code` which save the task event in time.

- `Collision_load` which represents the collision loads that will be applied for the collision.

- `Target_row` that specifies the choice of the target.

- `v_init` which is the initial velocity that will be the input of the Matlab function `first_collision` that models the collision

Visualization of targets and hand feedback is controlled by the remaining three blocks: `show_target`, `Hand_Feedback` and `Process_Video_CMD`. The `show_target` block creates a VCODE, which is a visual command to be processed by the `Process_Video_CMD` block. The `Hand_Feedback` block creates as well a VCODE for the hand feedback to be shown to the subject. The video commands are processed by the `Process_Video_CMD` block and this block outputs them in an appropriate format to the computer controlling the video[24].

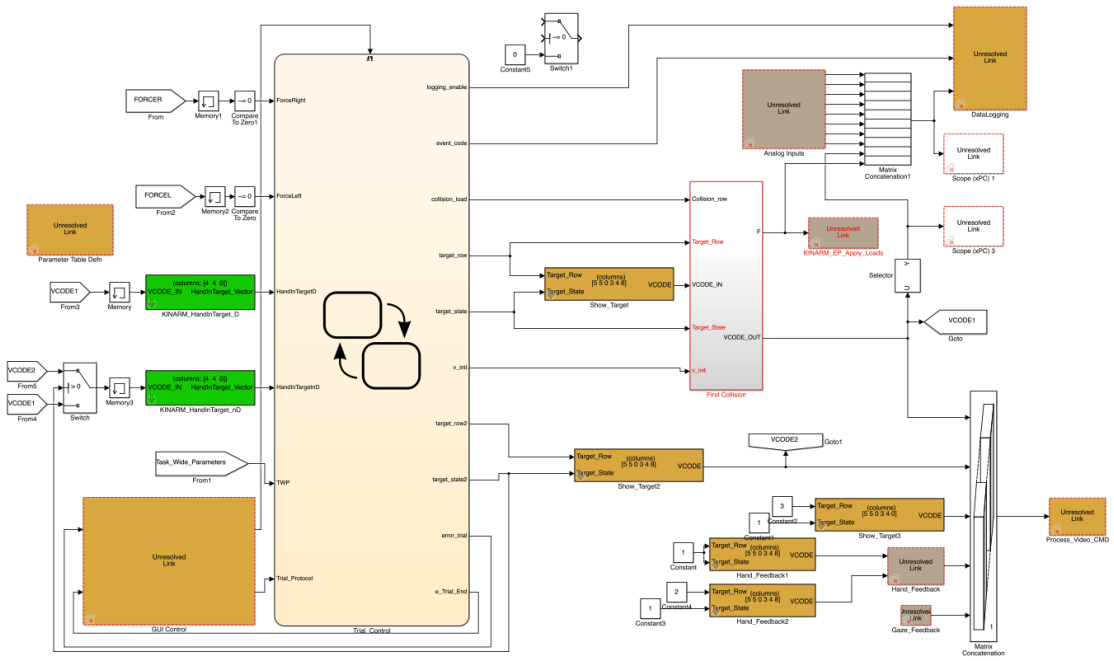

Figure 3.2: Simulink model

3.4 Implementation of the collision

The collision is mainly implemented in the Matlab function. The main goal of the Matlab function is to calculate and return the right and left forces that will be applied on the arms of the Kinarm robot due to the virtual collision. The data acquisition is done at 1kHz and the robot is controlled by a real time computer executing precisely the program of the experimental protocol. In others words, the Matlab function run every 1 ms. The previous values of the position of the target and its velocity have to be conserved during the simulation.
The outputs arms forces were computed following an equation of the collision that is described in the next section.

3.4.1 Detection of the collision

In order to apply the virtual impact force at the right or left hand, the exact moment of the collision needs to be detected. This happens exactly when the target hit the virtual representation of one of the two hands of the subject.
In order to detect the collision, the following equation is used to compute the distance from a point C(x_C,y_C) to a line with the equation $y = ax + b$:

$$d(C, y) = \frac{ax_C - y_C + b}{\sqrt{1 + a^2}} \tag{3.1}$$

Applying this to our case, the point C is the coordinates in x and y of the edges of the target as shown in figure 3.3. The equation of the line is the equation of line going through the coordinates of the edge of the virtual representation of the two hands. As the hand representation are inclined, the slope of the line is equal to $tan(\alpha)$ for the left hand, and the opposite for the right hand $-\tan\alpha$. Edges of the hand representation are calculated with respect to their center. It is the same for the target edges which are given by :

$$\begin{aligned} tlx &= x_t - \frac{t}{2}\sin\alpha \\ tly &= y_t - \frac{t}{2}\sin\alpha \\ trx &= x_t + \frac{t}{2}\cos\alpha \\ try &= y_t - \frac{t}{2}\cos\alpha \end{aligned}$$

with tlx, tly, trx and try that respectively represent the x coordinate edge of the target when target moves towards the left hand, y coordinate edge of the target when target moves towards the left hand and inversely when the target moves towards the right hand. x_t and y_t are the x and y position of the center of the target with respect to time.
For the hand edges:

$$hlx = lhx + \frac{l}{2}\sin\alpha$$
$$hly = lhy + \frac{l}{2}\cos\alpha$$
$$hrx = rhx - \frac{l}{2}\sin\alpha$$
$$hry = rhy + \frac{l}{2}\cos\alpha$$

with hlx, hly, hrx and hry that respectively represent the x coordinate edges of the hands' representation when target moves towards the left hands' representation and y coordinate edges of the hand when target moves towards the left hand and inversely when the target moves towards the right hand.

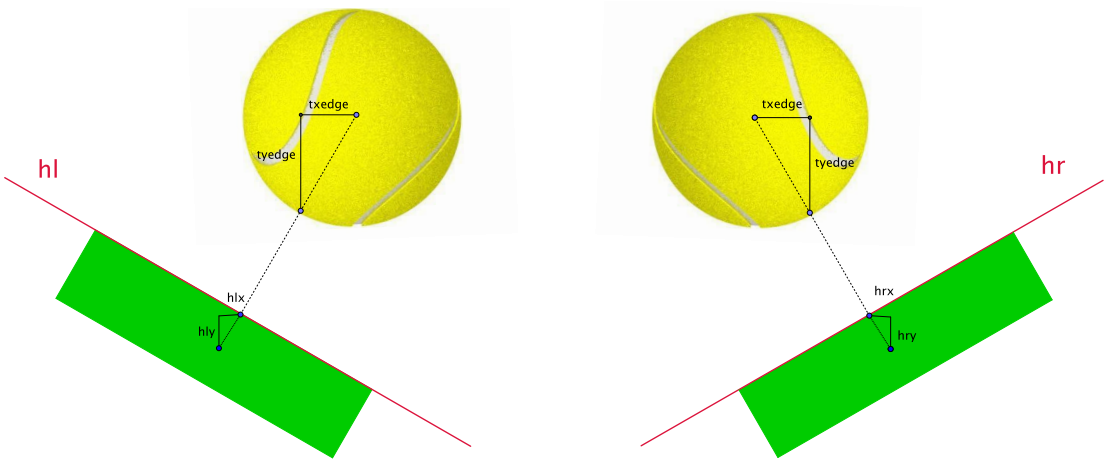

(a) Left handle (b) Right handle

Figure 3.3: Distance from the handle to the target. If this distance is positive, the collision not yet occurred. Inversely if it is negative, the collision occurs.

If the distance between the line and the edges of the target is negative,the target is below the line and the collision is detected. Inversely, if the distance is positive, the object is above the line and there is no collision. The force in the robot arm is activated when the distance between the line and the target is negative.

3.4.2 Modelling of the passive collision

To compute the force to applied in the robot arms, the collisions are modeled as passive collisions and are represented as elastics collisions. Kinetic energy is conserved in such a shock [27],[28]. It has been decided to represent the hand-target contact with a spring model shown on figure 3.4. One would represent it with a Kelvin-Voigt model, having a viscous element in parallel. However, the damping term dissipates too much energy during collision. This is why only the

spring model is used. This model has a purely elastic behavior and follows Hooke's law :

$$F = -kx$$

that states that the force F needed to compress a spring by some distance x is proportional to that distance, with k the spring constant, the stiffness.

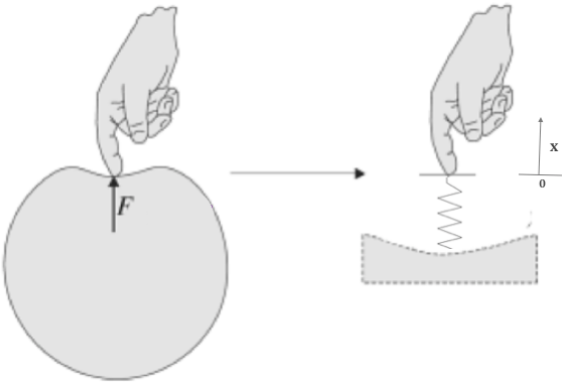

Figure 3.4: Elastic model, representing the contact between hand and target (adapted from [29]).

Thanks to this model, the contact force modeled on virtual hand is given by the following equation [29]:

$$F(x) = \begin{cases} -Kx & \text{for } x < 0 \\ 0 & \text{for } x \geq 0 \end{cases}$$

The velocity of the target after the impact is thus computed based on the mass of the target as well as the force calculated by the equation above, varying with respect to the initial velocity of the hand. In dynamics, a restitution coefficient occurring during inelastic collisions is defined. This coefficient takes values from 0 to 1 respectively for a perfectly inelastic collision, where all the kinetic energy is dissipated and for an elastic collision without energy loss [30]. In our case, the restitution coefficient will be equal to 1.

The target velocity depends on contact force, itself depending on hand velocity that will also be responsible of the value of the force applied on the hand at the impact. The target velocity after the impact will thus follow the following equations :

$$v_{tx} = \sum_t \frac{F_x(x(t))}{m_t} \Delta t$$
$$v_{ty} = \sum_t \frac{F_y(x(t))}{m_t} \Delta t$$

that states that the target velocity after the collision depend on contact force calculated in each direction, the target mass m_t and the delta time Δt equal to 1 ms. The total target velocity after the collision will therefore be given by $v_{total} = \sqrt{v_{tx}^2 + v_{ty}^2}$.

Chapter 4

Results

4.1 Grip and load force profiles

In the experiment participants produced collisions against six different targets with different masses and stiffness constants (see table 2.2). To analyze the adaptation of the grip force to novel objects it is helpful to represent the typical traces of forces involved in collisions. This will allow us to observe the general behavior of grip and load forces in different conditions.

Grip forces profiles were recorded for all trials, including catch trials in which the dynamic interaction with the target is deactivated, to observe the applied force of thumb and index finger and to investigate their strategy to cope with impulse-like load force. Catch trials are very useful to understand the results that will be explained in the following sections.

Figure 4.1 illustrates the average grip and load forces profiles in the six experimental conditions for all participants. The vertical green line is positioned at contact (0 ms), where elastics forces were activated to trigger the simulated collision. Catch trials are represented with a dashed line.

First of all, it can be seen that there is a clear asymmetry in the thumb grip force (red line) and index grip force profile (blue line). It seems that the impact would be mainly taken up by the thumb rather than by the index. Also, two peaks of grip force are observed, especially for the stiff conditions (figure 4.1b, d and f). We can noticed that the first peak of the thumb normal force (in red) is always synchronized in time with the peak load force (in pink) (regression analysis, R = 0.68). In all conditions, maximal grip force occurs after the impact.

This asymmetry can be explained by the hand and arm posture induced by the spatial configuration of the setup. Indeed, the position of the hand is inclined by 32.66 degrees with respect to the horizontal axis (see figure 2.3). The role and nature of the second peak of grip force has not been identified. We hypothesized that it may be the predicted grip force peak

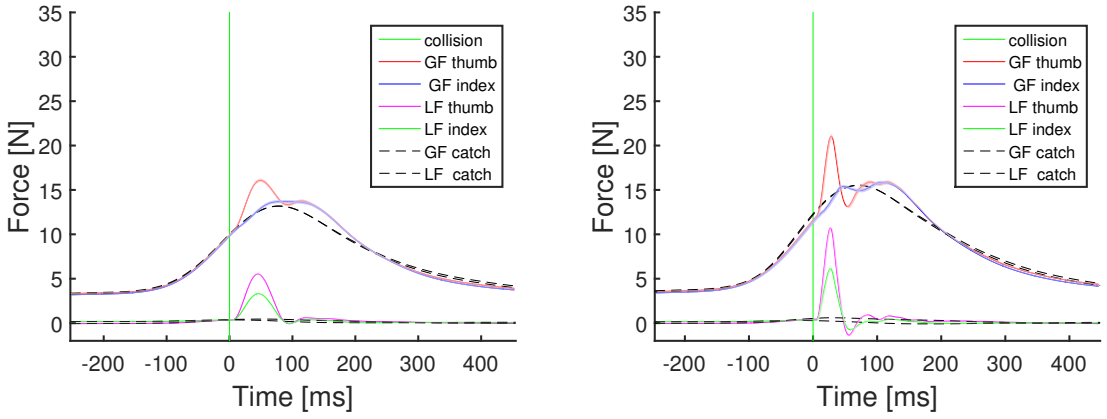

(a) soft m1

(b) stiff m1

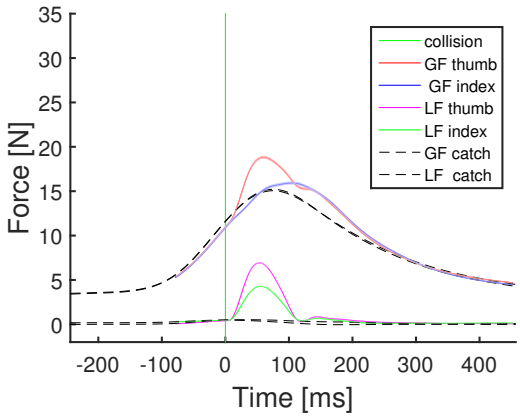

(c) soft m2

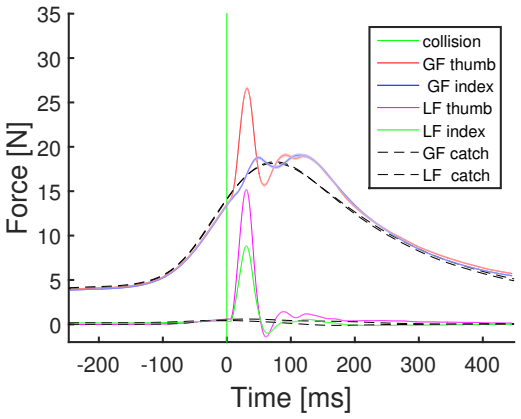

(d) stiff m2

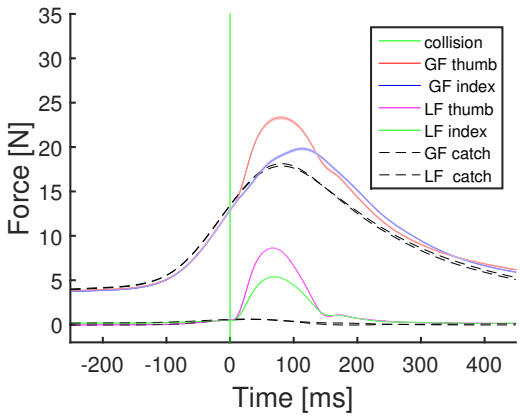

(e) soft m3

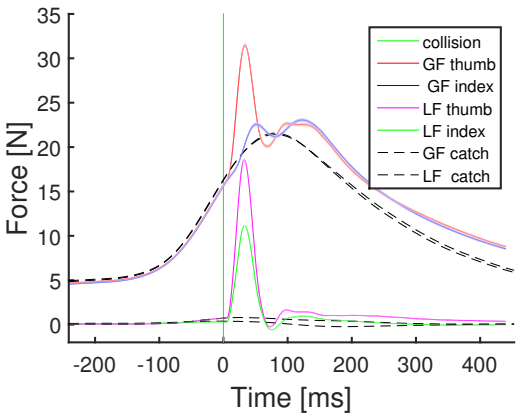

(f) stiff m3

Figure 4.1: Typical traces for the six different conditions showing the evolution of the grip and load force with respect to time. Collision is represented by the green vertical line at 0 ms. The thumb grip force and index grip force are respectively represented by the red and blue curve. Pink and green curves are respectively the thumb and index load forces. Dashed lines represent the grip and load force corresponding to catch trials. Shaded areas represent the stand error of the mean.

which manifests itself later than in a catch trial, influenced by the collision.

Importantly, catch trial profiles and regular trial profiles are very different. This difference is due to the mechanical component. Indeed, catch trials are trials for which collision loads are deactivated. The difference between normal trials and catch trials is the components related to the collision that we call mechanical component.

According to the different conditions the load force profiles evolves differently. Load forces peaks for low stiffness collisions are more spread over time than these for high stiffness collisions. As the grip force evolves with respect to the load force variations, the load force peak will be analyzed in the next section. Note that load force value at baseline is 0 N because no collision has yet taken place at that time.

4.2 Characterization of load force peak

As the grip force is synchronized with load force variations, it is interesting to first characterized the load force peak before analyzing the adaptation of the grip force. Indeed, grip force varies with respect the load force fluctuations. These fluctuations are directly induced by the mass and the stiffness constant of the target and can be explained by the integral of load force.

The load force profile depends on the target mass, the stiffness constant and the initial velocity of the target launched towards the subjects' hands. If the target mass increases the load force increases as well. However, the stiffness constant plays an important role in the modulation of the load force profile.

4.2.1 Peak impulse

As the load force impulse depends on the energy of the hand-target system, it is interesting to take a look at the impulse related to load force. Before the impact, energy of the system is given by kinetic energy. In the experiment, the target is always launched with the same velocity $v_i = 30\text{cm/s}$.

Impulse of load force in the six different experimental conditions are represented in figure 4.2. It is observed that these impulses of the same masses are not totally equal. Moreover the heavy/stiff condition is quite low compared to the heavy/soft condition. This can be explained by the fact that the integral of the load force was computed on an interval between two limits (see section 2.4). The lower one was defined as the value of the load force which reaches 10% of the maximal value of load force. The upper one is the value at which the maximal value reach 10% of its maximum after the peak. As a consequence, oscillations after the 10% of the peak are not taken into account in the integration (see figure A.1(a)).

Conditions	**Low** $GF_{contact}$		**High** $GF_{contact}$	
	Range [N]	**Mean [N]**	**Range [N]**	**Mean [N]**
Light/soft	6.05 - 8.1	5.6	8.1 - 42.57	14.15
Light/stiff	8.69 - 9.33	6.4	9.33 - 54	16.64
Medium/soft	6.66 - 9.15	6.3	9.15 - 49.85	15.5
Medium/stiff	10.3 - 11.6	7.9	11.6 - 53.9	19.1
Heavy/soft	8.6 - 11.1	7.6	11.1 - 48.4	18.2
Heavy/stiff	11.9 - 14.09	9.35	14.1 - 57.5	22

Table 4.1: Range of high and low grip force at contact.

Theoretically, energy for a perfect system without loss of energy is constant for the same mass. However, in the experiment that is not the case. Since the arm moves due to the collision energy is transferred to it and not given back to the system. Indeed, because of the arm impedance, load force impulses measured were smaller. The difference between impulse load force can thus be explained by the fact that the system variable depending on the damping of the arms'subjects. Integrals of load force for a same mass are not equal but their values are still close. Indeed, a high stiffness constant reduces the extend of load force profile in time and as a consequence, load force peak has to be higher to keep the integral of load force close to the integral of load force resulting in soft collisions.

Interestingly, we showed on figure 4.3 that the integrals of load force were higher when grip force before contact, $GF_{contact}$, was higher in all experimental conditions. Indeed, integral of load force when the grip force before contact is high is significantly ($p < 0.001$) different from integral of low grip force before contact. Inversely, when $GF_{contact}$ is low, the load force integral is smaller. At first, this result seems surprising because there was no difference between impact intensity inside a same condition. High grip force at contact and low grip force at contact were determined with respect to the median grip force of each participant before contact. Ranges of low and high grip force at contact are listed in table 4.1.

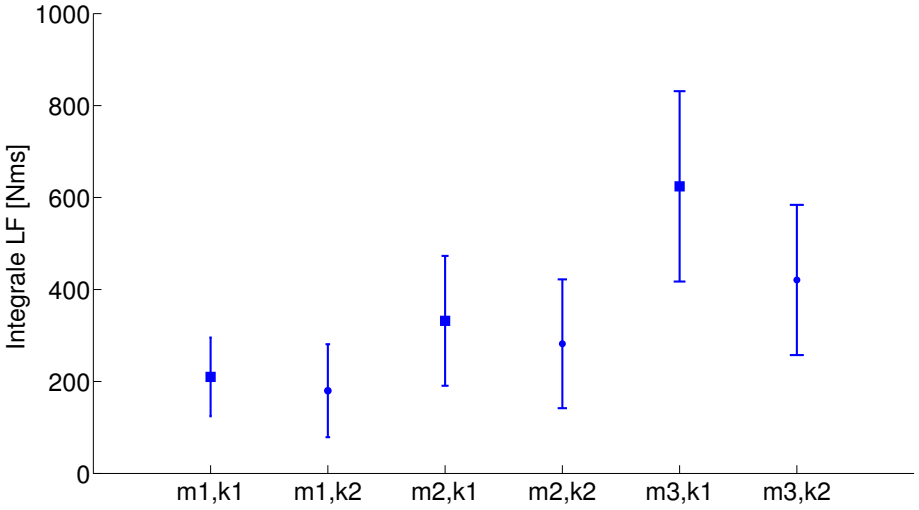

Figure 4.2: Integral of load force for each condition. Blue squares represent the soft conditions although circles represent stiff conditions. All values are given as mean ± SD

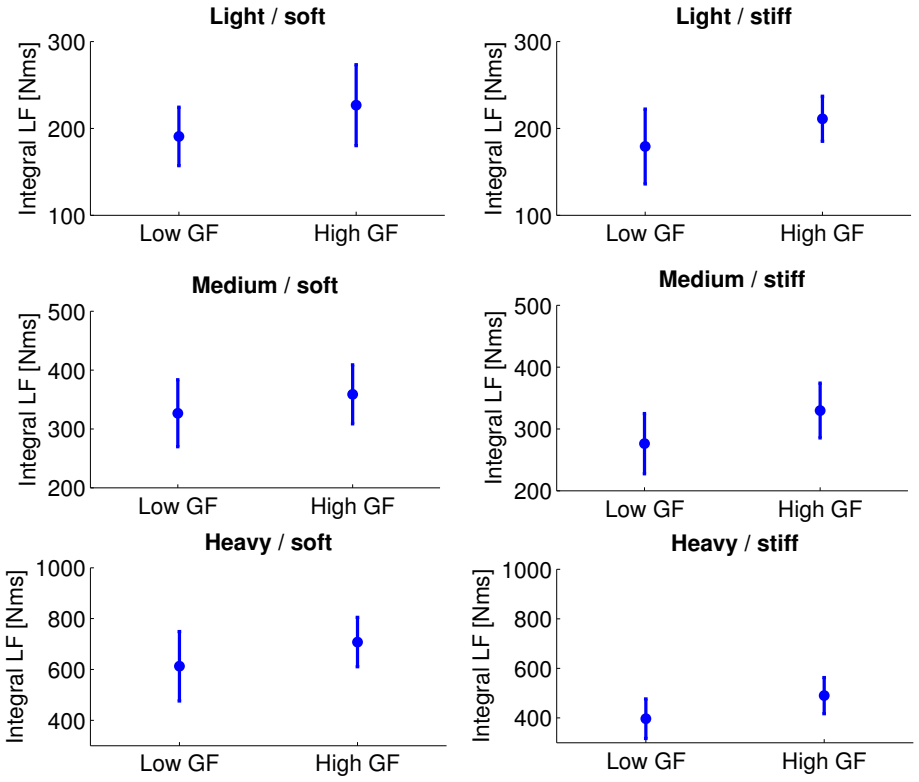

Figure 4.3: Integral of load force after contact for high and low grip forces at contact. Low and high grip forces were partitioned according to the median grip force for each participant. Values are given as mean ± SD.

4.3 Grip force control

It has been seen on the typical traces that there is a huge asymmetry due the orientation of the handles and we hypothesized that the impact would be mainly taken up by the thumb. We suggested that this asymmetry is caused by a mechanical component and not by a predictive mechanism, as it is absent in trial in which no collision occurs. However, as we want to investigate the predictive component of the grip force, we have to identify and extract this mechanical component.

4.3.1 Mechanical component

When facing a collision, the grip force profile after the impact reflects a mixture between an anticipatory response and a purely reactive response, which results from the feedback response to the collision triggered by mechanoreceptors [15]. According to some studies [9], reactive response occurs 100 ms after the impact. However, we saw on figure 4.1 that the first peak of thumb grip force (in red) occurs $\pm$ 30 ms after the impact, which is too quick to result from changes in reactive muscles activity. We hypothesized that it would be a mechanical component, resulting from mechanical interactions due to collision.

To identify the nature and the reason of its presence, this mechanical component was separated from the predictive component. To highlight the mechanical component in the experiment, a linear regression which estimates the predictive component of normal trials was used, based on the grip force and its derivative just before contact (see section 2.4.1 for details). The mechanical component of the trial is thus the difference at the moment of the load force peak between the value of the normal trial and its predictive value (see figure 4.4).

As the mechanical component is only present when load force is applied, we investigated the correlation between this component and the load force peak. For this part, we focus on the grip force force of the thumb. Indeed, this component is, at first, more identifiable on thumb profile than index profile and thus qualitatively less complex to investigate.

Figure 4.5 shows the mean mechanical component with respect to the mean load force of each condition. We can clearly find a correlation between the mechanical component and the load force. The higher the load force the more important is the mechanical component. However this is the correlation between the different conditions. We also can see that the variability of the mechanical component is very high (max SD = 5 N). This variability may be due to the deviation angle from the initial position of the handle at the impact, as it is not mechanical fixed. This possible correlation is studied and it is found that the mechanical component is correlated with the deviation angle especially when the stiffness constant is high (k_2: R = 0.55, k_1 : R = 0.31).

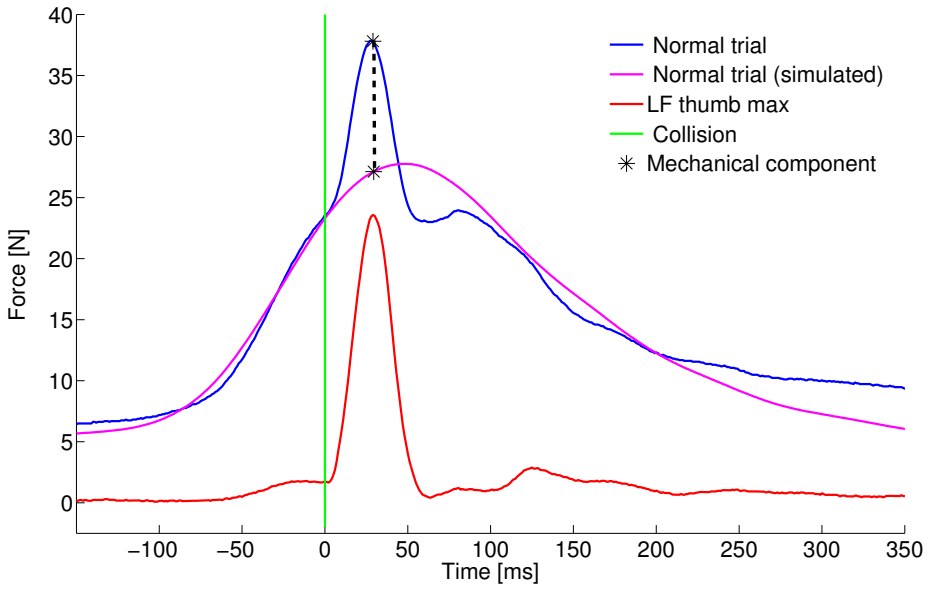

Figure 4.4: Example of one trial of the heavy/stiff condition of a subject. Figure show the thumb grip force in blue, thumb load force in red and the profile of the simulated normal trial. Black dashed line represent the incremental component related to the impact.

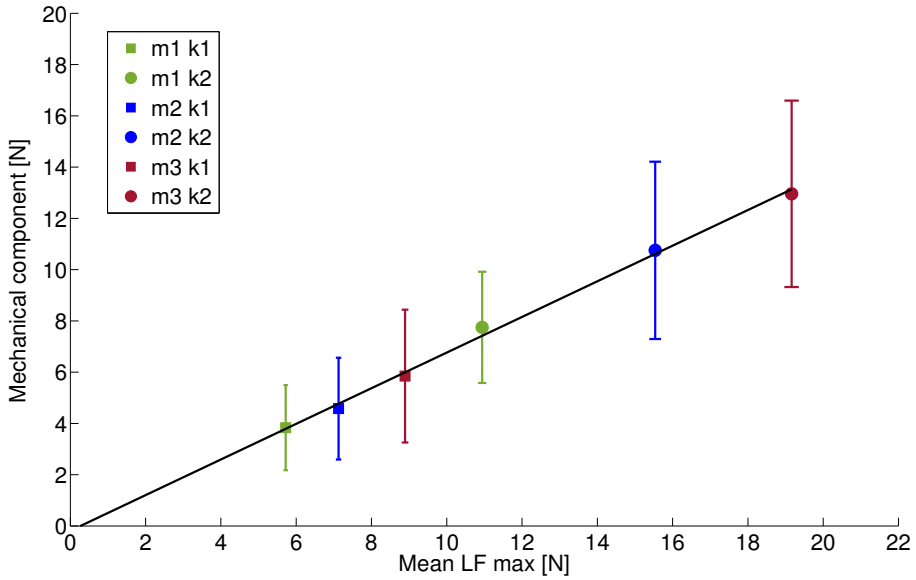

Figure 4.5: Mechanical component with respect to the mean maximal load force. Squares represent the soft conditions while circles represent the stiff conditions. Green, blue and red bars show respectively the light, medium and heavy conditions. Value are given as mean ± and error bars represent the standard deviation of the mechanical component.

4.3.2 Predictive control

The aim of the work is to know how the timing and intensity of grip force predictively adjust to novel object dynamics. Therefore, in this section, we computed the predicted component of grip force with the linear regression and the predicted component before the collision. For this section, only the second collision to sixth are investigated. The grip force response to the first collision is not predicable and hence discarded for the following analysis. The adaptation of grip force to the first collision will be studied in the next section 4.3.3.

Intensity and adaptation of grip force

Catch trials are helpful to understand and identify the predictive component of the grip force. Thanks to catch trials in which the dynamic interaction with the target is deactivated on randomly selected trials, we could measure the predictive component of the force profiles. This component is not a simple reflex and the consequence of collision since it was absent in specific experimental conditions when unpredictable load were applied to hand-held object [8]. Therefore, pure anticipatory and predictive component of grip force lies in catch trials. For this reason, a linear regression based on catch trials was used to estimate the predictive component of grip force in normal trials in order to extract the mechanical component from the analysis. In that way, we could observed how intensity of grip force adjusts to a novel object.

The task in this experiment is to wait for collision target while stabilizing the handle in hand. The trajectory of the target is visible for the subjects. In consequence, participants can predict the time of the target impact. As a result, a predictive mechanism is taking place and grip force increases progressively in anticipation of the occurrence of the impact.

The anticipative grip force was measured for all the experimental conditions as well as all participants on figure 4.6(a) (in blue). It is defined as the value of grip force measured at the moment when subjects begin to apply their grip before the collision. This component of grip force purely predictive because the collision has not occurred yet. We found that the values of the anticipatory grip force are correlated with the values of the grip force at contact ($r = 0.78$) and evolves in a same way. However, the time at which the subject starts to grasp appears to be fixed at 113.25 ± 4.35 ms before the collision. Therefore, subjects do not grasp earlier or later when facing different impact intensities but they begin to grasp with a higher or lower grip force.

When the subjects already had one collision, the impact intensity for the next collision was known. For the next collision, intensity of grip force were correlated to the mass and stiffness of the collision. In addition, the value of grip force at contact is only a predictive component of the grip force. As explained in the section 2.4 data analysis, it is thanks to the grip force just before contact and its derivative that the grip force maximum of the grip force's predictive component can be estimated.

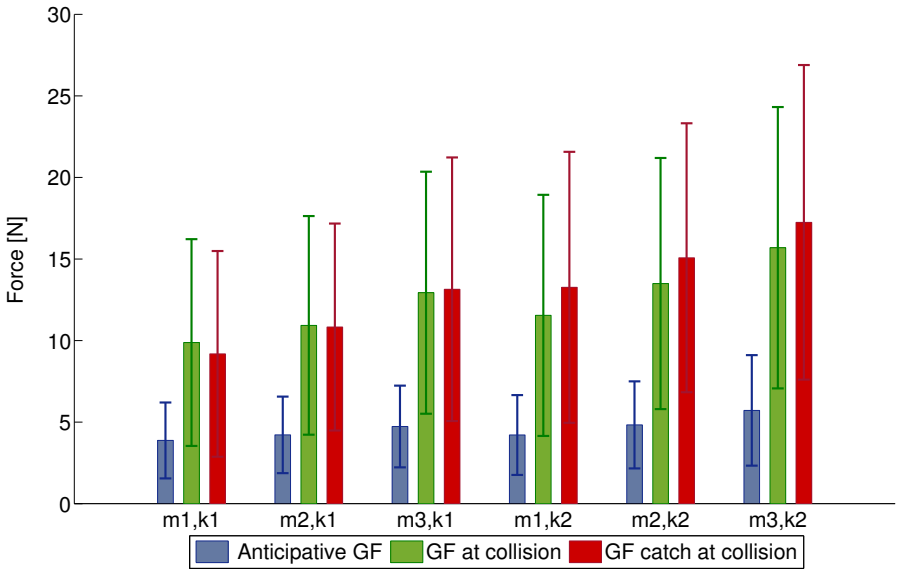

(a) Mean values of grip force before collision

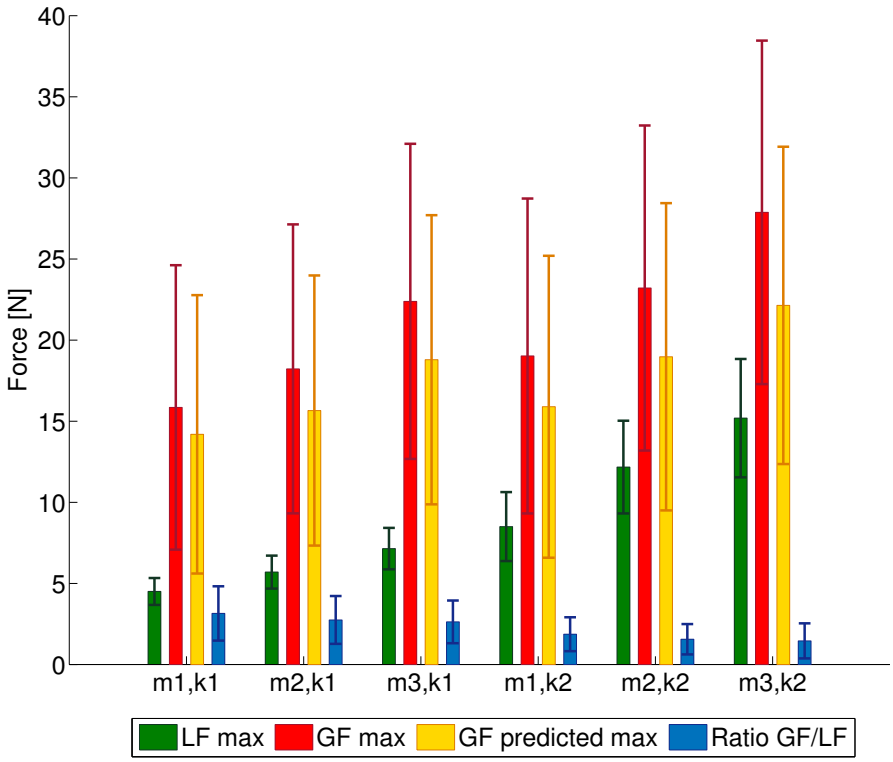

(b) Mean values of grip and load force after collision

Figure 4.6: Mean values of grip and load force for all participants through the six conditions. Figure a) shows the value of the anticipative grip force before the collision, the value of the grip force just before the collision and the value of the grip force for catch trials before the collision. Figure b) shows the value of the maximum load force the maximum grip force of normal and catch trials and finally, the ratio between the grip force maximum and load force maximum. In all graphs, values are given as the mean ± SD and are averaged on all the participants.

On figure 4.6(a), we can see the grip force at contact for the normal trial (in green) and the grip force at contact for the catch trial (in red). As the difference between the two kinds of trials is the lack of mechanical reaction due to the collision which has not occurred yet, the grip force at contact should not be different for both of them. This result is confirmed in figure 4.6(a) ($p = 0.6$). Moreover, participants expected a stronger impact in conditions with higher mass and stiffness constant, as evidenced by the increases of grip force at contact across conditions.

Figure 4.6(b) shows the average maximum grip force for the normal trial (in red), average predicted grip force maximum representing the predictive component of grip force (in yellow), average maximum of load force (in green) and the ratio of the predicted maximum grip force with respect to the load force maximum (in blue). It can be seen that the grip force is modulated with respect to the load force. As already said, the load force profile depends on its maximum value and on its duration. For stiff collisions, duration of load force if shorter than soft collision. Therefore, we can observe two tendencies on maximum grip force values and thus on ratio GF_{max}/LF_{max} related to stiffness constants. Indeed grip and load force ratio of soft targets and stiff targets are significantly different ($p = 0.0016$).

Interestingly, the maximum of the predictive component of the grip force follows the same evolution than the maximum grip force of normal trials. Their difference in value lies in the mechanical component.

Timing of grip and load force peaks

Several studies have proved that the grip force peaks were not synchronized with the load force peak in collision phase [12] [10]. We therefore investigated if the stiffness of the target modulates the latency of the grip force peak. Does the grip force occur later in stiff than in soft collisions? A more delayed grip force peak in the stiff collision would allow a more efficient damping of the instabilities coming from the collision [15].

To test it, we look at the time of grip force peak with respect to time of collision are reported in the figure 4.7. It is important to note that the grip force profile used to report the time is the predictive component of grip force computed by linear regression in normal trials as we want to investigate the predictive component. In this way, it is possible to observe that the latency of maximum grip force (in blue) relative to contact is fixed at 79.9 ± 5.56 ms across the different conditions. However, the latency of load force peaks is not fixed in time (in red). Again, there are two tendencies for those latencies with respect the to the stiffness constant k_1 and k_2 ($p < 0.001$). Load force peak latency for soft collisions (27.44 ± 3.71 ms) is almost double of that one of stiff collisions (52.8 ± 9.86 ms). This would be explained by the fact that the load force profile of soft collision is more spread in time than this of stiff collision. Its maximum occurs therefore later than in stiff collisions.

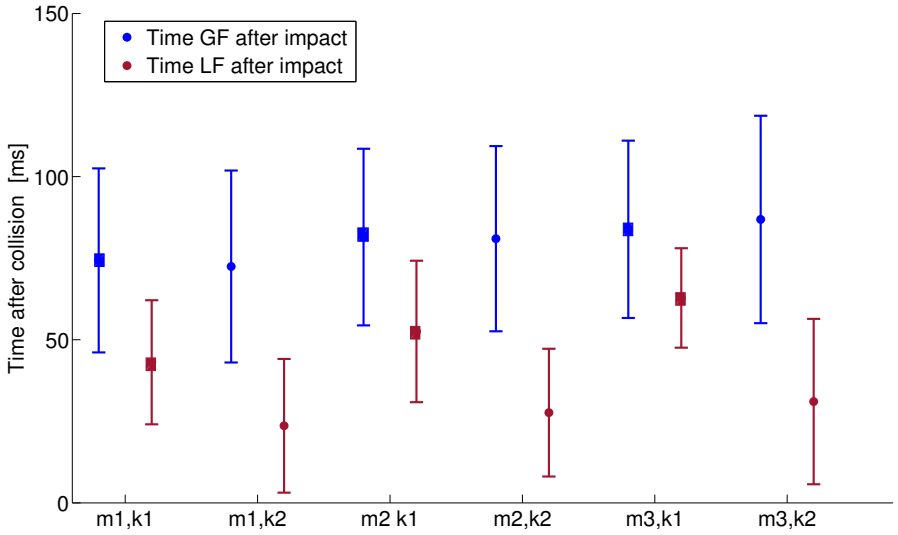

Figure 4.7: Mean time occurrence of load force peaks and predicted values of grip force. Blue squares and red squares represent the time after collision at which the maximum of grip and load force occurs for the soft collisions. Inversely, blue and red circles represent the time after collision at which the maximum of grip and load force occurs for the stiff collisions. Values are given as mean ± SD of all participants.

4.3.3 Influence of previous trials

Participants have to produce six collisions with the target for one specific impact intensity. In total, there were six different impact intensities randomly distributed throughout the experiment. As a consequence, all subjects do not have the same experimental conditions in the same order. In this section we investigated the value of grip force for the first collision, with a non predictable impact intensity, and the influence of the different intensities of impact of the previous trials. In other words, we investigate the effect of the sixth collision of the previous condition on the first collision of the actual condition i.e. influence of heavy/stiff target collision before the first collision with the light/soft target.

Figure 4.8 shows the mean maximal load force of the 6th collision (in green), called LF_{6th}, of the previous trials of different conditions before the condition of the actual trial. Mean maximal grip force of the 1rst collision of the actual condition (GF_{1rst}) is also represented (in blue) as well as its corresponding mean maximal load force (LF_{1rst} in pink). Load forces of previous conditions are represented for all the six actual conditions (m_1,k_1/$m1$,k_2,...) on the figure 4.8. Grip force maximum values are estimated by linear regression to eliminate mechanical components (see section 2.4.1 for details).

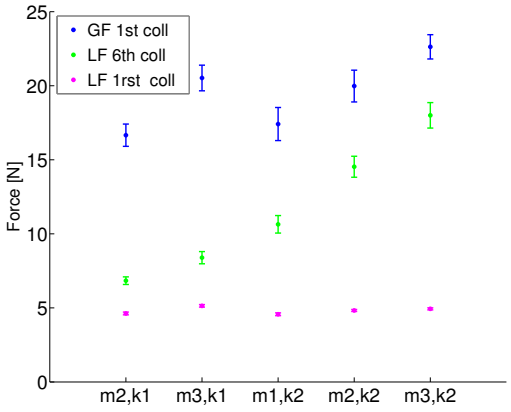

(a) Actual condition : light/soft (m_1,k_1)

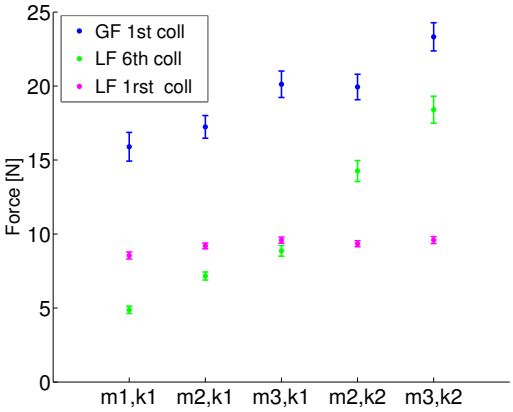

(b) Actual condition : light/stiff (m_1,k_2)

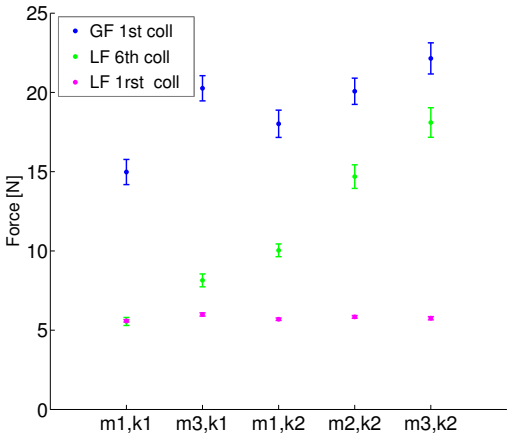

(c) Actual condition : medium/soft (m_2,k_1)

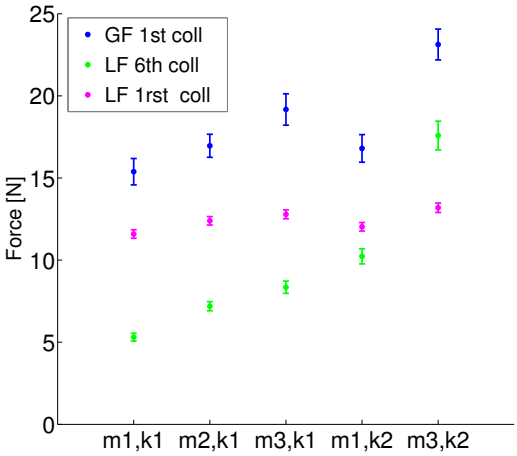

(d) Actual condition : medium/stiff (m_2,k_2)

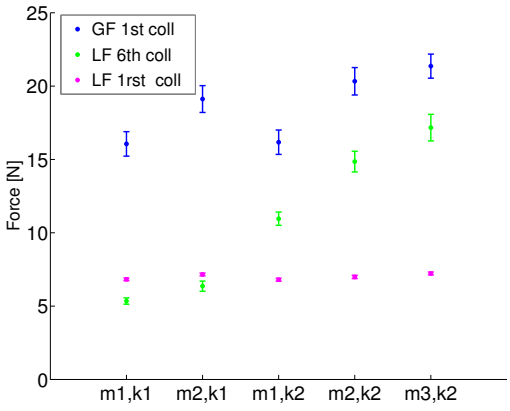

(e) Actual condition : heavy/soft (m_3,k_1)

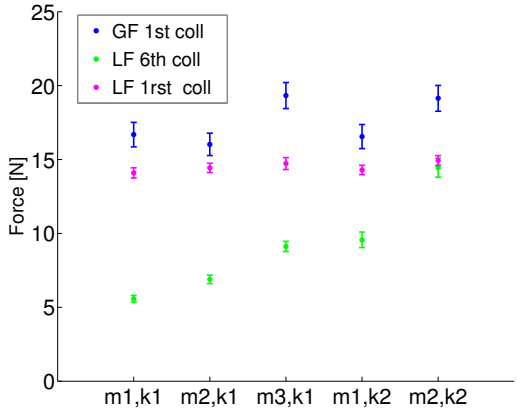

(f) Actual condition : heaby/stiff (m_3,k_2)

Figure 4.8: Influence of the previous impact intensity on the first collision of the actual condition. Grip force and load force of the first collision of the actual condition are respectively represented in blue and pink. Load force of the sixth collision of previous condition is represented in green. Values are given as mean ± SD.

It can be seen on figure 4.8(a) that grip force of 1rst collision of the actual condition is correlated with previous 6th collision load force (R = 0.86). Indeed, we can notice that when LF_{6th} is the load force corresponding to heaviest mass with the higher stiffness constant (m_3,k_2), GF_{1rst} of condition m_1,k_1 is higher than for LF_{6th} corresponding to m_1,k_2. This evidences a correlation between GF_{1rst} and LF_{6th}. However there is a lower correlation between the grip force of the 1rst collision and its corresponding load force. The same observations can be made on figure 4.8(b), 4.8(c), 4.8(d) and 4.8(e). In all these figures, GF_{1rst} is also highly correlated with the previous load force LF_{6th} (R = 0.92,R= 0.82, R= 0.9, R= 0.71).

In addition, taking a look at the figure 4.6(b), we can see the load forces corresponding to the six different conditions. The difference between these two figures is that the figure 4.8 shows the GF_{1rst} and LF_{1rst} for single condition (same impact intensity) instead of figure 4.6 which shows these corresponding to six different conditions (different impact intensities). Interestingly, GF_{1rst} on figure 4.8 evolves in a similar way as the grip forces on figure 4.6. This provides a second evidence for the correlation between GF_{1rst} and LF_{6th}.

Influence of previous trials on the last condition m_3,k_2 is a little bit different from the others (figure 4.8(f)). Indeed, as the LF_{1rst} is higher than other load forces, GF_{1rst} of m_3,k_2 seems less influenced by LF_{6th}. It could be explained by the correlation between GF_{1rst} and LF_{1rst} which is higher than for the others conditions (R = 0.73).

4.4 Grip force learning

Subjects were required to grasp the handle with a precision grip and wait for the collision with different impact intensities due to different masses and stiffness constants of the target (see experimental conditions table 2.2 for details). For one condition, i.e m_2,k_2, 30 series of six consecutive collisions occurred, alternately to the left and right hands. One of the objective of this work is also to study the adaptation of grip force and the learning at grip force adjustments through the six consecutive collisions. Can we rapidly learn to apply the right grip force to a novel object? As the mechanical component depends only on mechanical interactions as target masses, stiffness and orientation angle, the maximum grip force reported is the value of the predicted grip force, computed by the linear regression.

4.4.1 Grip force adaptation and learning in a collision task

Figure 4.9 shows the mean maximum value of grip force for all participants for the first, second and sixth collision of the six conditions. We can see a decrease of the maximum grip force for the light/soft (m_1, k_1), light/stiff (m_1, k_2) and medium/soft conditions (m_2, k_1). No significantly difference was found between the grip force maximum of the first collision of the medium/stiff condition (m_2, k_2) and the sixth collision ($p > 0.1$). The same result was found for the heavy/soft condition (m_3, k_1).

Interestingly, the grip force increases significantly for the heavy/stiff condition. It can be explained by the fact that this target was very heavy and stiff and participants did not expect such a target. Their reaction was probably to grasp harder to cope with this high impact target.

The mean maximum grip force is represented for each collision of each condition on figure 4.10. Thanks to a multiple comparison test, it is possible to determine from which collision we can consider that participants have learned to apply a correct grip force with respect to the corresponding load force.

For all conditions, except medium/stiff and heavy/soft conditions (figure 4.10(d) and 4.10(e)), the grip force of the first collision is significantly different from the grip force of the sixth collision ($p < 0.001$). That provides evidence that the subjects learns and adapt to the object dynamics during these conditions. For the light/soft condition, maximum grip force is significantly different until the third collision. After that, the value of grip force is not significantly different anymore ($p > 0.01$). In other words, participants needed three collisions to provide the correct force in response to the applied load force. However it takes only two collisions for the light/stiff, medium/soft and heavy/stiff conditions to directly apply the right grip force corresponding to collision dynamic. As we can see on figure 4.10(d) and 4.10(e), no evolution of grip force is observed for collisions of the medium/stiff and heavy/soft conditions as no significant difference was found ($p > 0.05$).

Remember that participants had 30 series of 6 collisions randomly distributed during the all experiment. The grip force learning between the 30 series of 6 collisions was also investigated. Nevertheless, no significantly grip force adaptation was observed between those series.

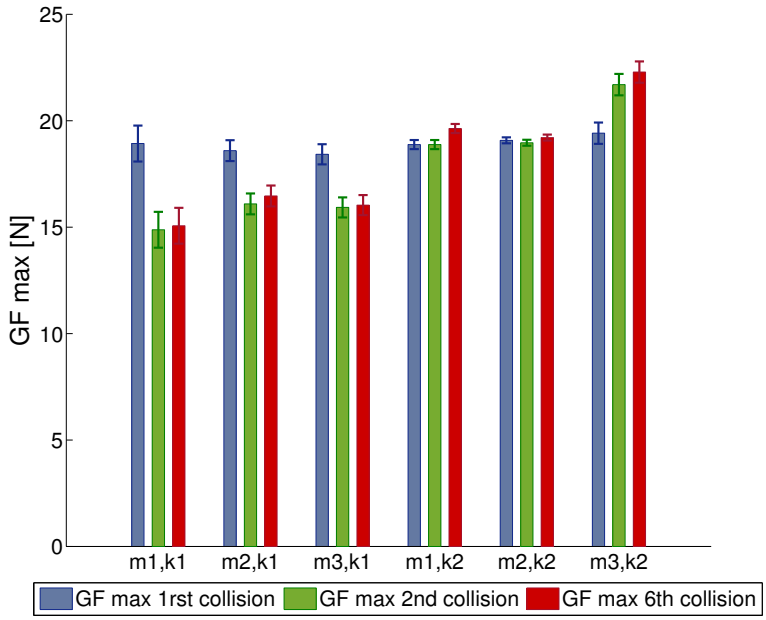

Figure 4.9: Evolution of mean maximum grip force through collisions for all participants. Blue, green and red bars represent respectively the maximal grip force for the first, second and sixth collision of one condition. Error bars represent the standard error of the mean across trials.

4.4.2 Evolution of the grip and load force ratio

To better understand why no learning effect between the medium/stiff and heavy/soft conditions was observed, we analyzed the mean ratio between maximum GF and LF. In that way, we could observe if the apparent non-adaptation is the consequence of an already good ratio GF/LF at the first collision.

Figure 4.11 shows the evolution of the mean ratio between maximum grip and load force throughout collisions. Again, as in section 4.3.2, we can clearly observe two tendencies for the ratio between GF_{max} and LF_{max} ($p < 0.001$) following the two stiffness constant k_1 (figure 4.11(a)) and k_2 (figure 4.11(b)). The mean of the ratios between the maximum grip force and maximum load force for the six collisions is represented with a pink dashed line. This average line will be helpful to compare the ratio from different conditions in order to see if subjects provided directly the correct ratio of grip and load force. In addition, we can notice ratio GF/LF for the medium /stiff condition (m_2,k_2) and the heavy/soft condition (m_3,k_1) are very closed and nearly superimposed on the average line. For the others stiff and soft conditions, it can be seen that the curves of GF/LF ratios converge towards the average line.

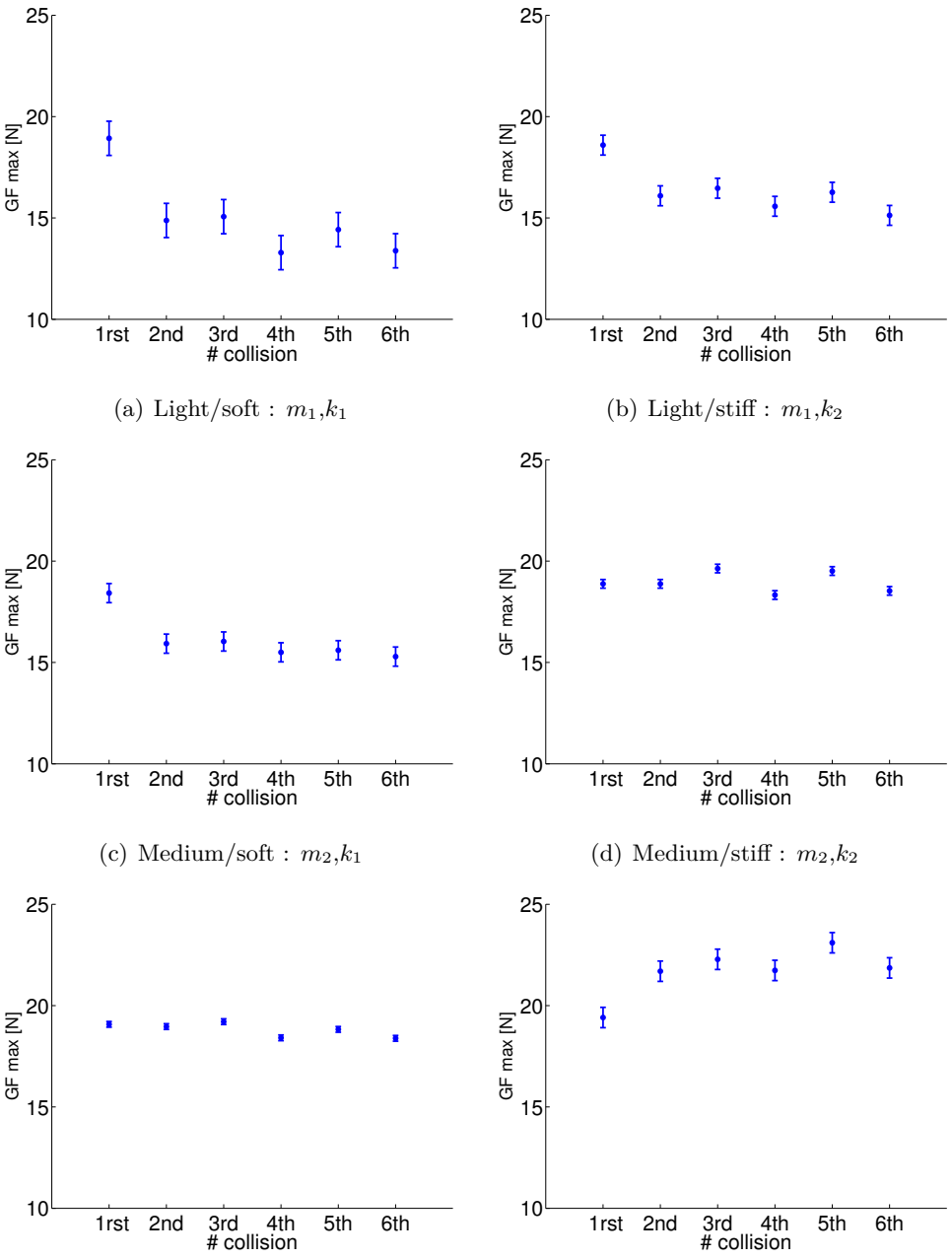

(a) Light/soft : m_1,k_1

(b) Light/stiff : m_1,k_2

(c) Medium/soft : m_2,k_1

(d) Medium/stiff : m_2,k_2

(e) Heavy/soft : m_3,k_1

(f) Heavy/stiff : m_3,k_2

Figure 4.10: Mean of the maximum grip force per collision and per condition for all participants. Error bars represent the mean ± SEM.

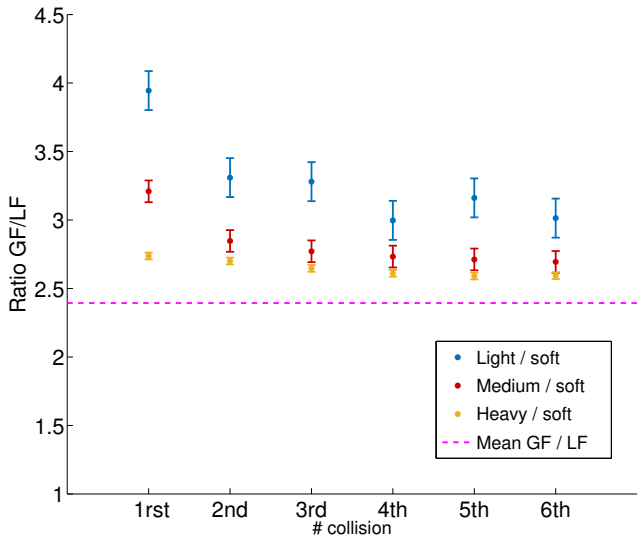

(a) Soft collisions

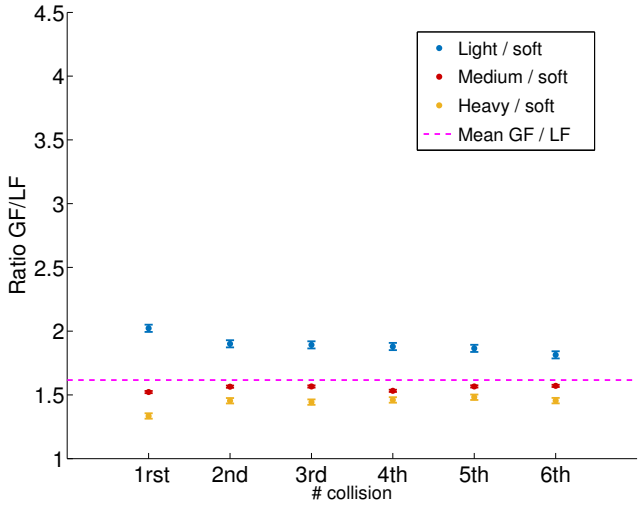

(b) Stiff collisions

Figure 4.11: Ratio between the grip force maximum and load force maximum of each collision for a) soft collisions and b) stiff collisions. Dashed pink line is the ratio between the maximum grip and load forces of the first collision. Values reported in the traces are mean ± SEM.

Chapter 5

Discussion

Modulation between grip and load force is a strong indicator of a prediction control provided by internal models. Various authors reported anticipatory adjustments of grip force for different forms of load force. In hands movements, the tight coupling between grip and load force demonstrates the predictive control of grip force with respect to the load force [14]. Here we assessed the predictive mechanisms underlying grip force control in a task involved passive horizontal collisions with different masses and stiffness of targets. Participants were asked to wait for collisions while stabilizing the collision.

Mechanical and predictive component

Grip force response to collision is composed of a mechanical component resulting from mechanical interactions induced by the collision and a predictive component provided by an internal model. This mechanical component was extracted from the predictive component thanks to catch trials and a linear regression based on the grip force at contact and its derivative. We saw that the mechanical component was highly correlated with the load force peak. Indeed, the higher the load force is, the higher the mechanical component is. This provides an evidence that the mechanical component is related to the impact intensity and is induced by mechanical interactions. Moreover, the value of the mechanical component represents about 68% of the mean proportion of load force . The energy of the impact corresponding of the thirty last percentages would be absorbed by the grip force applied before the collision.

However, the variability of the mechanical component allows us to think that there was an other parameter linked to its presence. As the handles used for the experiment are not mechanically fixed, we investigated its relationship with the deviation angle at the impact time. This deviation angle is defined as the difference between the initial position of the handle inclined of 32.66 degree with respect to the horizontal axis and the inclination of the handle after the impact. A high correlation between the mechanical component and the deviation angle was found with stiff collisions rather than soft collisions. This would be explained by the fact that in

case of stiff collisions the intensity of the impact is higher and less extended in time. Following the impact, subjects would be more likely to deviate from their initial orientation. In addition, the asymmetry of the thumb grip force profile is related to the mechanical component and could be a direct consequence of the initial inclined position of the handle (32.66 degrees). It would be interesting for a further study to investigate the relation between the orientation angle of the handle and the presence of the mechanical component as well as its intensity .

We also questioned about the nature of this component. Investigations of the force response immediately after the perturbation demonstrated the first increase in grip force occurring almost immediately after the perturbation (30 ms), which is too quick to result from changes in reactive muscles activity. This increase likely reflected mechanical interactions, such as viscoelastics forces resulting from collision or the Poynting effect, characterized by a force normal to the direction of a shear stress applied to tissue with nonlinear elasticity, such as the skin. However range of values of this mechanical component may be too high to explain its entire nature only with the Poynting effect (< 2N) [31].

Intensity of predictive grip force

To investigate how the grip force adjust predictively when facing collisions with different impact intensities, the mechanical component was extracted from normal trials in order to focus on predictive component of the grip force profile and to avoid biased responses induced by the impact. First, the predictive behavior of grip force before the collision was studied. Grip force increased progressively in anticipation of the occurrence of impact and reached a maximum 79.9 ± 5.56 ms after the impact. Similarly, Turrell et al. (1999) found a maximum grip force around 100 ms after the impact in their collision experiment. Moreover, the anticipatory grip force adjustments were time-fixed at 120 ms before collision for all subjects in all conditions and it was found that the values of these predictive adjustments were related to the impact intensity. Subjects would grasp higher or lower depending on impact intensity but not earlier before collision. As these results were found for the anticipatory grip force for the second to the sixth collision (the first collision not predicable has been discarded from this analysis), this provides an evidence of that anticipatory modulation of grip force is dependent on the history of manipulation of the last trials.

After the first surprisingly collision, subjects had the opportunity to get an idea of the impact intensity. It was observed that the larger the mass was, the stronger the grip force. Same observations were made for the stiffness constant. It results that the predictive system adapts the predictive component of grip force with respect to the impact intensities. Indeed, also when no impact occurs, the predictive component of grip force is also modulated with the load force which should have been applied. Lower ratio between grip and load force was found for stiff

collisions. In others words, we would apply less grip force for stiff collisions. This would be explained by the fact that frequencies of the destabilizing forces in stiff collisions are higher and are sustained if the grasp interface is stiff (if the grip force at contact is high) [15]. Therefore, there is a clear advantage to adsorb the vibrations at contact by providing a moderate or lower grip force with respect to the high load force.

For the first collision, a correlation was found between the grip force of the first collision and the load force of the previous trials. Indeed, grip force was modulated with respect to the load force of the previous condition. Influence of previous trials has been shown in some studies with classical grip-lift tasks. Such a modulation with respect to previous trials has been described as a sensory motor memory effect for fingertips or a typical anticipatory behavior resulting from a prediction of the consequence of a movement [9].

Adaptation of grip force for the six collisions was also studied inside each condition. The results show that the curve of the GF/LF ratios converged towards the mean ratio of GF/LF. For most of all conditions, this convergence was reached at only the second collision. This suggests a rapid learning effect and a rapid adaptation of internal model. However, for two conditions (medium/stiff and heavy/soft) we observed and apparent non-adaptation through collisions. This results in the fact that subjects already provide the right ratio at the first collision as the curve of these ratio was closed or nearly superimposed the averaged line.

Latency of grip force peak

Implementation of catch trials helps us to clearly measure the predictive component of the grip force and to evidence a pre-programmed grip force peak $\simeq 80$ ms after the impact. Interestingly, this grip force peak occurs after the impact and not at the time of collision, when a peak of load force occurs and when the risk of slippage is the highest. We thus investigated whether latency of the predictive component of grip force was more delayed or not with respect to the target stiffness. Results showed that this peak of grip force was time-fixed at 79.9 ± 5.56 ms across the different conditions. A study of Bleyenheuft and al. (2009) [9] provides an explication about the reason about the delayed presence of grip force peak after target collision. They hypothesized that the delayed peak allows mainly the natural damping properties of the skin to absorb high frequencies in the destabilizing forces to stabilize the grasp. They also found that once the peak grip force is reached, more than 70% of the destabilizing vibrations are already damped out by the skin properties. In addition, some studies show that the anticipatory increase in stiffness just before ball impact involved generalized muscle co-activation, which serves mainly to increase stiffness magnitude [32]. This is confirmed by our results which show that the higher grip force is, the higher the integral of load force representing the mechanical constraints. Indeed, when grip force increases the stiffness of the contact between hand and target, the damping of the destabilizing forces resulting from the collision are reduced. The modulation of grip force

at contact is thus important. A compromise is needed between maximizing the damping and ensuring a safe grasp after the complex transients [9].

Load force variability

Finally, for all trials of the experiment, we noticed a high variability of the load force inside one condition between participants. At first sight it seems surprisingly because all impacts have the same intensities within a condition. We saw that the load force integral varied with respect to the grip force before contact. Indeed, a high grip force at contact would demonstrate a higher stiffness at contact. This stiffness at contact influencing the integral of load force was variable with respect to the grip force applied by the different subjects. This would provide one hypothesis that would explain the variability of the load force. Moreover, vibrations resulting from the impact may be transmitted to the arm and this one would damped and restored the shock differently following the different subjects. Indeed, if the displacement of the arm/hand is high, it would indicate a higher loss of energy in the arm resulting in a lower restoring load force.

Chapter 6

Conclusion

In conclusion, the results presented in this work demonstrate that when subjects had some sensory feedback of the dynamic of the different intensity of impacts resulting from previous trials, this knowledge could be used to update internal forward models and, thus, enable subjects to provide grip force for the forthcoming trials. Indeed grip force that was scaled to load force increases in all conditions whether the anticipation of grip force before collision or the predictive component after collision. Therefore, the motor control required for generating a preparatory increase of grip force before the impact and an increase of grip force after the impact is thus planned to optimally stabilize the object around the collision. In addition, predictive adaptation of grip force for the six collisions, show us the rapidity of acquisition of a suitable forward internal model to the assigned task.

On the other hand, the fixed latency of the peak grip force provides an evidence for a preprogrammed grip force peak and this short latency results from a compromise between a safe grasp after the impact and an absorption of high frequencies in the destabilizing forces. This may suggest that the central nervous system controls the impedance of the hands through grip force to account for the dynamics of the task [15].

Finally, this work provides an overview of the predictive behavior of grip force using the functionality provided by the Kinarm robot and shows us the ability of the predictive system to adapt to novel conditions and environment.

Bibliography

[1] Roland S Johansson and J Randall Flanagan. *Tactile sensory control of object manipulation in human*, volume Handbook of the Senses : Vol.5-Somatosensation. Elsevier, 2007.

[2] Mitsuo Kawato. Internal models for motor control and trajectory planning. *Current opinion in neurobiology*, 6, 1999.

[3] Daniel M. Wolpert and J. Randall Flanagan. Motor prediction. *Current Biology*, 11, 2001.

[4] Paul R Davisdson and Daniel M Wolpert. Widespread access to predictive models in the motor system : a short review. *Journal of Neural Engineering*, 2, 2005.

[5] R.C.Miall and D.M.Wolpert. Forward model for physiological motor control. *Neural Networks*, 9, 1996.

[6] Olivier White. *The role of gravity in dextrous manipulation: a driving force rather than a perturbation.* PhD thesis, Université catholique de Louvain, Juin 2007.

[7] Sarah-Jayne Blakemore, Daniel Wolpert, and Chris Frith. Why can't tickle yourself? *NeuroReport*, 11, 2000.

[8] R.S. Johansson and G. Westling. Programmed and triggered actions to rapid load changes during precision grip. *Experimental Brain Research*, 71, 1998.

[9] Yannick Bleyenheuft, Philippe Lefèvre, and Jean-Louis Thonnard. Predictive mechanisms control grip force after impact in self-triggered perturbations. *Journal of Motor Behavior*, 41, 2009.

[10] Y. N. Turrell, F-X. Li, and A. M. Wing. Grip force dynamics in approach of a collision. *Experimental Brain Research*, 128, 1999.

[11] Dennis A Nowak, Joachim Hermsdörfer, Katrin Rost, Dagmar Timmann, and Helge Topka. Predictive and reactive finger force control during catching in cerebellar degeneration. *The Cerebellum*, 3, 2004.

[12] D.J. Serrien, P. Kaluzny, and U. Wicki. Grip force adjustments induced by predictable load perturbations during a manipulative task. *Experimental Brain Research*, 124, 1998.

[13] R. Martyn Bracewell, Alan M. Wing, Harriet M. Soper, and Kristen G. Clark. Predictive and reactive co-ordination of grip and load forces in bimanual lifting. *European Journal of Neurosciences*, 18, 2003.

[14] J. Randall Flanagan and Alan M. Wing. Modulation of grip force with load force during point-to-point arm movements. *Experimental Brain Research*, 95, 1993.

[15] O. White, J.-L. Thonnard, A. M. Wing, R. M. Bracewell, J. Diedrichsen, and P. Lefèvre. Grip force regulates hand impedance to optimize object stability in high impact loads. *Elsevier*, 189, 2011.

[16] Thibault Giard. *Grip force adaptation to static and dynamic torques during object manipulation.* PhD thesis, Université catholique de Louvain, 2016.

[17] Benoit Delhaye. *Skin mechanics involved in dynamic touch.* PhD thesis, Université catholique de Louvain, 2014.

[18] Westling G and Johansson RS. Factors influencing the force control during precision grip. *Experimental Brain Research*, 53, 1984.

[19] Frederic Danion, Jonathan S. DIamond, and J. Randall Flanagan. The role of haptic feedback when manipulating nonrigid objects. *Journal of Neurophysiology*, 107, 2012.

[20] J. Randall Fanagan and Roland S. Johansson. *Encyclopedia of the Human Brain : Hands Movements*, volume 2. Elsevier Sciences, 2002.

[21] Anne-Sophie Gissot-Augurelle. *Feedback and feedforward processes underlying grip-load force coupling during cyclic vertical arm movements.* PhD thesis, Université catholique de Louvain, 2003.

[22] Arsalis. *KINGRIP Calibration Certificate and Accuracy Report*, 2015.

[23] bkin technologies. `http://bkintechnologies.com`. Online; October 25, 2015.

[24] BKIN technologies. *Creating Tasks Program For Dexterit – E^{TM}*, 2015.

[25] Mathworks. Simulation et approche model-based design.

[26] Mathworks. Stateflow: Modélisez et simulez la logique de décision à l'aide de machines d'état et de diagrammes de flux.

[27] Hugh D. Young and Roger A. Freedman. *University Physics with modern physics*, volume 1. Pearson, thirteenth edition, 2012.

[28] Rod Cross. The bounce of a ball. *American Journal of Physics*, 67, 1999.

[29] M.Mihelj and J.Podobnik. *Haptics for Virtual Reality and Teleoperation*, volume 64. Springer, 2012.

[30] Rod Cross. The coefficient of restitution for collisions of happy balls, unhappy balls, and tennis balls. *American Journal of Physics*, 68, 2000.

[31] Frédéric Crevecoeur, Jean-Louis Thonnard, Philippe Lefèvre, and Stephen H.Scott. Long-latency feedback coordinates upper-limb and hand muscles during object manipulation tasks. *eNeuro*, 3(1), 2016.

[32] Etienne Burdet, d David W. Franklin Rieko Osu2k a, Theodore E. Milner, and Mitsuo Kawato. The central nervous system stabilizes unstable dynamics by learning optimal impedance. *J mot behav*, 41 (5), 2011.

Appendix A

Data processing and analysis

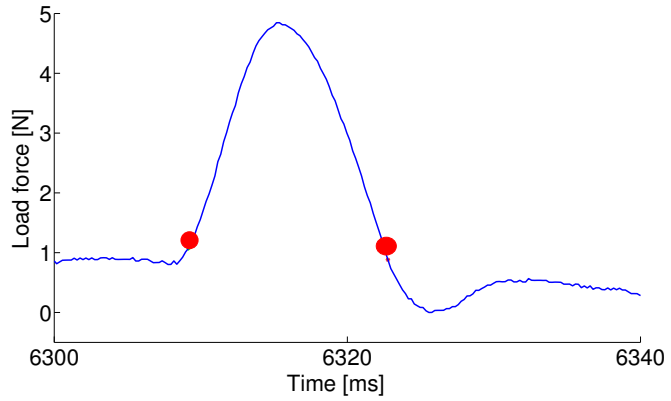

(a) Limits of the integrale of the load force profile

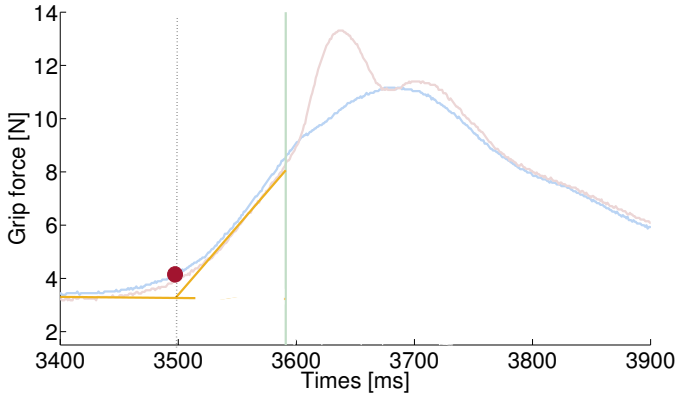

(b) Value of anticipative grip force

Figure A.1: a) Integral of load force computed on an interval between two limits. The lower one was defined as the value of the load force which reaches 10% of the maximal value of (in red) load force. The upper one is the value at which the maximal value reach 10% of its maximum after the peak b) The time (dashed line) of anticipation of grip force is taken at the intersection of two lines. These lines are the fit on the first value of grip force and the fit on the slope before the collision. The value of grip force at the anticipation is the value of grip force at the anticipation time (circle in red). Collision is represented by the green line.

Appendix B

Influence of previous trials

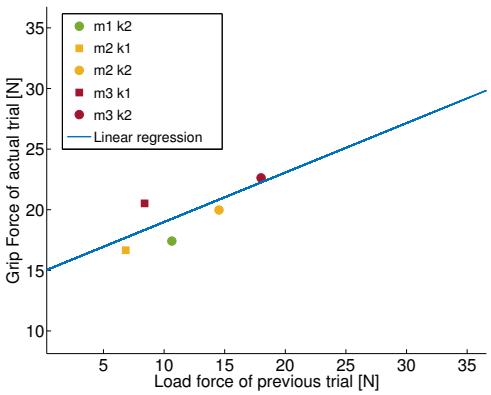

(a) Actual condition Light/ soft with respect to LF of previous trials of others conditions

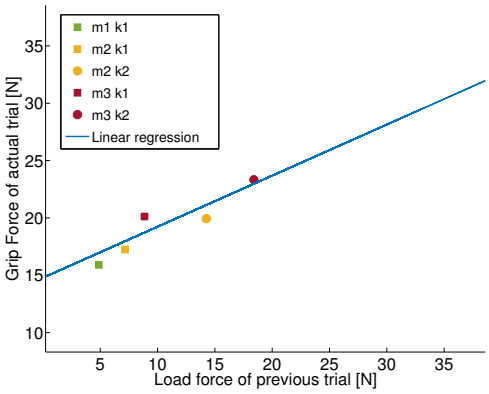

(b) Actual condition Light/ stiff with respect to LF of previous trials of others conditions

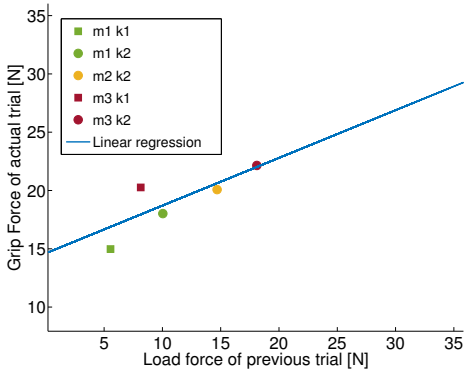

(c) Actual condition Medium/ soft with respect to LF of previous trials of others conditions

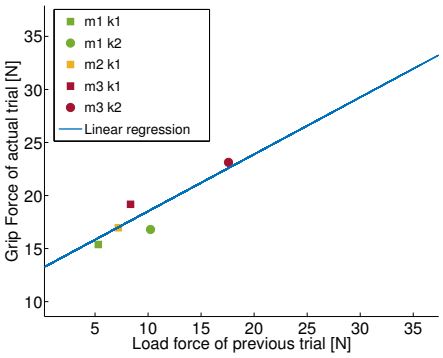

(d) Actual condition Medium/ stiff with respect to LF of previous trials of others conditions

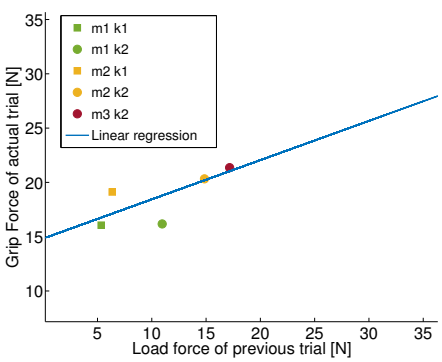

(e) Actual condition Heavy/ soft with respect to LF of previous trials of others conditions

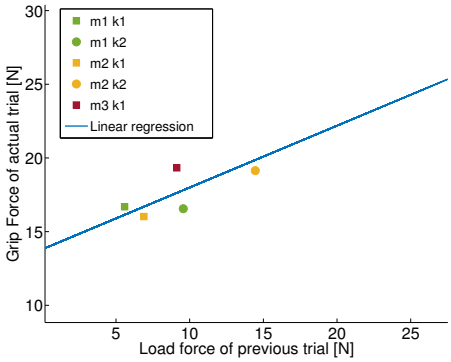

(f) Actual condition Heavy/ stiff with respect to LF of previous trials of others conditions

Figure B.1: Grip force of the 1rst collision of the actual condition with respect to load force of the 6th collision of the previous trial. Squares represent soft collisions and circles represent stiff collisions. The three different colors are related to the different masses : green for m_1 (2kg), orange for m_2 (4kg) and red for m_3 (8kg). Blue line is the linear regression of these values.

Rue Archimède, 1 bte L6.11.01, 1348 Louvain-la-Neuve **www.uclouvain.be/epl**